PhD

PROGRAM IN TRANSLATIONAL AND MOLECULAR MEDICINE

DIMET

UNIVERSITA' DEGLI STUDI MILANO-BICOCCA
SCHOOL OF MEDICINE AND SCHOOL OF SCIENCE

Identification of early pathophysiological events underlying venous bypass coronary stenosis by a mechano-biology approach

Coordinator: Prof. *Andrea* Biondi

Tutor: Dr. *Maurizio* Pesce

Dr. *Francesca* Prandi
Matr. No. 744998

XXVI CYCLE
ACADEMIC YEAR
2012-2013

Ai miei genitori,
vi voglio bene

Table of Contents

Chapter I:

General Introduction

1. Coronary Heart Disease: Introduction to the clinical problem

Coronary Heart Disease (CHD) is an ischemic pathology affecting heart characterized by an insufficient supply of arterial blood flow to the cardiac tissue muscle. The insufficient blood supply is caused by formation of atherosclerotic plaques into the arterial vessels that vascularize myocardium (coronary arteries), over time the coronary lumen narrows and progressively reduces the flow of oxygen-rich blood to the cardiac muscle (ischemia).

Treatments of CHD are aimed at restoring the normal blood supply to the ischemic myocardium. These include Percutaneous Coronary Intervention (PCI) and Coronary Artery Bypass Grafting (CABG).
PCI involves non-surgical widening of the coronary arteries using a balloon catheter to dilate the vessel from within, after dilatation the arteries are maintained expanded by a metallic stent placed inside.
To the contrary, CABG is an open-heart surgical procedure during which a healthy artery or vein is grafted into the heart in order to bypass the narrowed portion of the coronary artery. This technique creates new path for arterial blood flow toward the heart muscle.

1.1. Epidemiology of Coronary Heart Disease

CHD is among the major causes of death in the western countries. On the basis of data from America Heart Association an estimated 15.4 million Americans ≥ 20 years of age have CHD (www.heart.org). CHD affects most men than women, indeed the total prevalence of CHD in the population is 7.9% for men and 5.1% for women. CHD makes up more than half of all cardiovascular events in ≤ 75 years of age. The risk of developing CHD grow during lifetime: after 40 years of age it increases to 49% for men and 32% for women and about 80% of people who die of CHD are >65 years of age. The actual number of deaths attributable to CHD is 27.1% in the United States of America (AHA computation).

1.2. Coronary Artery Bypass Grafting: a brief overview

In CABG, one or more coronary arteries are bypassed by an autologous vessel graft to restore normal blood flow to the ischemic heart.

Arteries or veins, taken from the patients itself, are used as conduits for CABG. The effectiveness of CABG in relieving symptoms and prolonging life is directly related to graft patency. Because arterial and venous grafts have different patency rates and modes of failure, conduit selection is important in determining the long-term efficacy of CABG.

Vessels commonly used as bypass grafts are the followings:

Mammary arteries: Internal Mammary Artery and Left Internal Mammary Artery (LIMA) are the most common bypass grafts as they have been shown to have the best long-term results. In most cases these arteries can be kept intact at their origin (they branch out from subclavian artery) and sewn to the coronary artery downstream the occlusion.

Saphenous veins (SVs): these veins are removed from lower limbs and grafted in reverse; they are anastomized proximally to the aorta and distally to the coronary artery below the site of blockage.

Radial artery: there are two arteries in the lower arm: the ulnar and radial artery. Most people receive adequate blood flow to their arm from the ulnar artery alone and will not have any side effects if the radial artery is removed and used as graft, preoperative tests determine if the radial artery can be used.

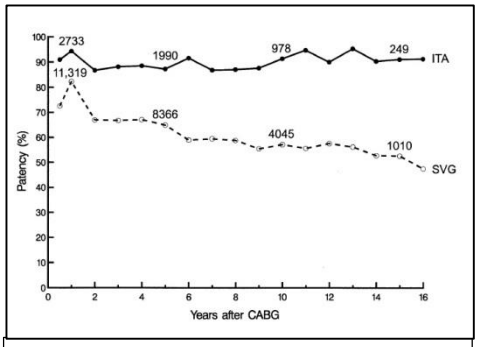

Figure 1.1 Patency rates of artery grafts (ITA, Internal Toracic Artery) is superior to patency of venous grafts (SVG).

1.3. Different conduits, different patency at post graft strategies

Reversed saphenous vein grafts (SVG) are commonly used in patients undergoing CABG. Their disadvantage is a declining patency with time: the patency rates is 88% early after grafting but decreases to 75% at 5 years and to 50% at ~12.5 years [1].

Moreover, at 10 years after CABG only half of SVGs have no angiographic evidence of atherosclerosis [1]. Unlike Saphenous Vein Grafts, grafts made with Internal Mammary Artery usually are patent for many years postoperatively (10 years patency > 90%).

The disadvantage of using arterial conduits is their spasm and eventually atrophy if used to bypass a coronary artery that is not severely narrowed [2].

1.4. Morphology of Vein Vessels

The structure of vein wall mimics that of arteries, as general structure is concerned: both vessel walls are composed of three distinct layers: the intima, the media, and the adventitia; these three layers are separated by the internal and external elastic layers (Fig. 2). The main cellular components of a vein wall in its normal state are endothelial cells (EC) and smooth muscle cells (SMC). ECs form a flattened monolayer on the elastic basement membrane (intima layer), and are thought to play an essential role in venous wall integrity and function. Smoot muscle cells are the main cell type present in the media layer just under intima layer; the adventitial layer is the outer part of vessel wall composed by fibroblast cells, *vasa vasorum* (micro vessels that give blood supply to the vessel wall) and nervous network in a matrix not compact. However, in the vein, cellular and fibrous components are significantly limited in number, particularly in the medial, leading to a vessel that is generally thinner than the wall of a comparable anatomic artery. Eph-B4 is a well-known marker that address venous vasculature development in embryo. Eph-B4 contributes significantly to the structural differences between arterial and venous wall thickness, as Eph-B4 limits mural cell recruitment [3], cell proliferation by ERK dephosphorylation [4], and vein wall thickness in mature tissue [5].

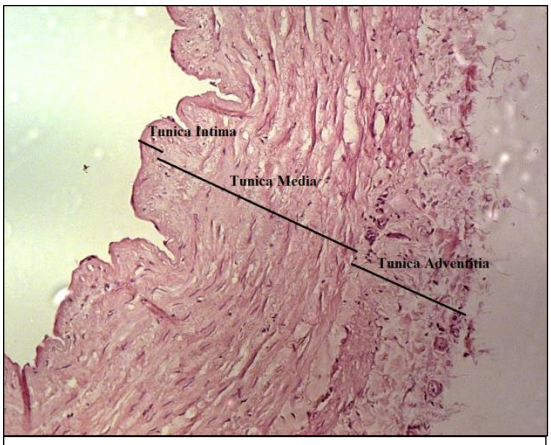

Figure 2. Histological image of a saphenous vein showing the tree layer that compose the vein vessel wall. Hematoxilin and Heosin staining.

In the normal physiological environment, the structure of the vein undergoes constant adaptation to flow and pressure loads. The venous wall is usually

exposed to a low pressure and low flow rate; consequently, its structure guarantees high adaptability for a constantly changing hemodynamic load. The compliance of the thin venous wall supports this adaptive flexibility to variable local blood volume, the vein physiologically adapts to its new environment via a transition of its venous wall structure.

1.5. Vein Wall Physiologic Signals

It is well known that healthy ECs produce the vasorelaxant prostacyclin (also known as PGI2) as well as endothelium-derived nitric oxide (NO) [6-8]. PGI2, produced primarily by cyclooxygenase, and NO, produced by nitric oxide synthase (NOS), work in coordinated fashion to prevent platelet activation, adhesion, and aggregation [9, 10]. NO is also known to be a negative conductor for the expression of chemical mediator secretion and inflammatory cell adhesion molecules ICAM-1 and VCAM-1 [11]. In early stages of vein graft adaptation, physiological low-concentration NO is known to have an important role for protecting the vascular wall from platelet-derived vasoactive substances and inflammatory responses [8, 12].
SMCs also play an important role in vessel wall homeostasis. In a normal venous environment, the interaction between SMCs and the extracellular matrix (ECM) promotes a quiescent state in the SMCs via endogenous molecules (TGF-β, heparin, and heparin-like-molecules) [6, 13-15]. Thus, the normal vessel wall is characterized by a low rate of cell turnover, both cell proliferation and apoptosis.

1.6. Saphenous Vein Graft Failure – Pathophysiology -

SVG failure is the main cause of repeated intervention by either CABG or PCI and is even more common than the progression of native coronary artery disease in patients undergoing CABG. In spite that SVG failure remains a significant clinical and economic burden, the majority of CABG procedures continue to use SVG [16]. The high incidence of vein graft failure has therefore led to the devise of graft surveillance programs to detect ‘failing’ grafts and efforts have focused on means to control the overall failure process [17].

Intimal hyperplasia (IH) is the cause of vein graft failure. IH is the vessel wall thickening with proliferation of smooth muscle cells and deposition of extracellular matrix in all layers of the vein graft, especially in the intima.

The etiology for all vein graft adaptation is initiated by **surgical resection** of the vein. During the vein harvest, nervous network of vein wall is disrupted, the adventitia layer is damaged and the *vasa vasorum* are resected; consequences of this disruption include tissue hypoxia as well as hyponutrition of vessel wall [18]. Vein graft hypoxia leads to the release of inflammatory cytokines, which have downstream impact in neointimal hyperplasia; for example IL-6 and IL-8 have been shown to be specifically released in this setting [19]. Since during harvesting the *vasa vasorum* and nervous network of the SVG are removed, the graft is dependent on nutrient and oxygen diffusion from blood stream. Adequate microcirculation is re-established only after some weeks after intervention. [20-23].
At the time of harvest, the quality of the saphenous vein may be poor, showing pre-existing non-symptomatic pathological conditions ranging from significantly thickened walls to varicosities. Between 2% and 5% of saphenous veins are unusable and up to 12% can be considered diseased which reduce the patency rate by one half compared to non-diseased veins [24].
The inevitable vascular trauma that occurs during SVG harvesting can also lead to damage to the endothelium and smooth muscle cells (SMCs) and thereby contribute to graft failure. Surgical manipulation and high-pressure distension to reverse spasm during harvesting leads to loss of endothelial integrity, rendering the SVG prone to subsequent occlusive intimal hyperplasia and/or thrombus formation [25]. Given the poor results of the common harvest of saphenous vein during CABG, surgeons adopted a new technique called “no touch” technique. It avoids high-pressure distension of the conduit preserving the endothelium and muscular fibers structure. The side effect of “no touch” procedure is the risk to run into graft bleeding since not all collaterals of the vein can be sutured [26].

In 2005, Mitra and colleagues reviewed the sequence of biological events in vein graft neointima formation [6]. They broadly classified the events

leading to neointima into five steps: 1) platelet activation and correlated events; 2) inflammation with leukocytes recruitment; 3) activation of the coagulation cascade; 4) SMC migration and 5) proliferation.
Clinically SVG failure can be divided into three temporal categories: **early** (0 to 30 days), **midterm** (30 days to 1 year) or **late** (after 1 year).

1.6.1. **Early SVG failure:** it occurs in 15% to 18% of VG during the 1st month [27, 28].
The transition from venous to an arterial environment with its higher wall shear stress and strain injures the vein graft endothelium. Injured endothelium acts as a theater for platelet events quite rapidly, within a minute after vein graft implantation. At the site of endothelial injury, exposed sub-endothelial matrix leads to the adherence and aggregation of platelets. Numerous cytokines and other bioactive substances are released by activated platelets [29]; for instance, adenosine diphosphate that activates the arachidonic acid synthesis pathway which produces thromboxane A2, a potent chemo-attractant and a SMCs mitogen [6, 30]. Several other growth factors and cytokines, such as PDGF, TGF-β, IL-1, IL-6, IL-8, and thrombin, are also known to come into play following platelet activation [31]. Under arterial conditions, the physiological venous tissue homeostasis that induced NO and PG12 production is disrupted contributing to enhance SMCs proliferation. The perioperative administration of aspirin as anticoagulant improves early (1 month) and 1-year SVG patency [32, 33]. Endothelial injury also activates the coagulation cascade. Thrombus formation at the site of injured vein graft endothelium is well known to contribute not only to promotion of acute phase but also to intimal hyperplasia formation in vein graft. Tissue factor (TF) is the key mediator of coagulation at the site of vessel wall injury when sub-endothelium is exposed to the circulating blood [6]. Downstream from initial phases of coagulation, coagulation factor Xa and PDGF released from activated platelets play a role in SMCs mitogenesis [45]. Circulating TF additionally is a known SMC proliferation agonist [46, 47].

1.6.2. **Midterm SVG failure:** during the subsequent weeks after implantation, leukocytes recruitment and the inflammatory response play primary roles in vein graft progress. Chronic inflammation in the graft wall is initiated by adherence molecule expression following platelet activation at the injured endothelium site. Activated leukocytes then migrate into the graft vessel wall; molecules such as MCP-1 [35], ICAM [36, 37], Mac-1 [38], and GPIbα [39] mediated this process. TGF-β overexpression is sustained until the late phase of vein graft adaptation; instead, MCP-1 production is active primarily during the early phase of vein graft adaptation and diminishes after 1 week, as observed in an experimental animal model [40]. Expression of adherence molecules and molecules for leukocytes recruitment are essential events in the early, midterm phase of graft adaptation. Indeed, by blocking MCP-1 receptor using gene transduction in a mouse vein graft model, a 51% volume reduction in neointimal hyperplasia was appreciated [35]. Leukocytes migration is an important factor in neointima development: Peppel and colleagues showed that 60% of the neointima area of ROSA26 mice vein graft model was derived from cells extrinsic to the graft [41].

Resection of SV from the lower limb causes not only the cut of *vasa vasorum* and nerves but also the disruption of lymphatic vessels that serve the vein wall. Thus, the return of interstitial fluid and inflammatory cells from vein graft tissue to lymphatic system is blocked; with the consequence that inflammatory exude remains in the graft, making the inflammatory situation worse.

Given the role of inflammation in the neointima formation, suppression of

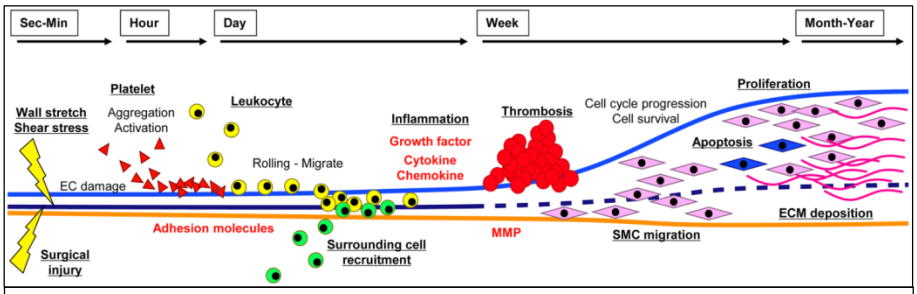

Figure 3. Time-course of vein graft neointimal formation. EC, endothelial cell; SMC, smooth muscle cell; MMP, matrix metalloproteinase; ECM, extracellular matrix. *Akihito Muto, Circ J. 2010* August

the immune reaction is a theoretical option in the treatment of pathologies associated with neointimal hyperplasia. Flavonoids, which are known to have anti-inflammatory, anti-allergic, and anti-oxidant effects, also attenuates rat vein graft neointima formation through the dowregulation of PDGF-BB and TNF-α [42]. Rapamycin, the most well analyzed immunosuppressive agent, inhibits LPS-dependent TNFα release from human SV SMCs in culture [43]. In fact, in vivo perivascular rapamycin application by pluronic gel showed dose dependent reduction of neointimal hyperplasia due to decrease inflammatory cell infiltration and increase cell apoptosis [44].

1.6.3. Long term vessel remodeling leads to **late SVG failure;** it is characterized by progression of intimal fibrosis at the cost of a reduction in cellularity, which is mainly due to SMCs apoptosis [34, 37, 41, 48]. After 1 year, most SVG stenosis is due to atherosclerosis. Although vein graft atherosclerosis is accelerated compared to arteries, evidences show that a fully evolved plaque only appears after 3 to 5 years of implantation [49, 50].
Bio-attractive factors play an important role in the late phase of vein graft neointimal formation [40]: for example, IL-8 is a known neutrophil chemoattractant, IL-1, IL-6 and TNF-α, in association with reactive oxygen species, numerous growth factors, and proteolytic enzymes, modulate the chronic inflammatory responses [51].
During vein graft adaptation, ECM degradation is a necessary process for SMCs migration into the neointimal layer. Matrix metalloproteinases (MMPs) are key enzymes in ECM degradation and remodeling in injured vessel walls [52]. For example, via alteration in ECM components, MMP-9 and MMP-2 induce SMCs proliferative phenotypes and subsequently accelerates neointimal hyperplasia [53-55]. Furthermore, tissue inhibitor of metalloproteinases (TIMP) treatment of vein grafts consistently attenuates neointima formation in mouse model [54]. Interestingly, in vivo adenoviral MMP-3 transfection reduces rabbit vein graft stenosis and neointimal hyperplasia [56]. Therefore, the functions of MMPs are complex, with overlapping or bidirectional interactions, and comprehensive clarification is necessary for an integrated understanding of MMP activity during vein graft wall remodeling.

1.7. Adventitial Contribution to Vein Graft Disease

For many years, the tunica adventitia has been regarded as a collagen rich connective tissue poorly cellularized, which received no great appreciation as the intima and media layers in vessel pathology. Now the importance of adventitia layer is changing. In fact, recent studies show that the adventitia functions as a dynamic compartment for cell trafficking into and out of the vessel wall, it participates in growth and repair of vessel wall, and it mediates communication between the intima/medial layer and the local tissue environment. The adventitia contains lymphatic vessels, autonomic nerves, microvasculature that nourish the vein wall; it contains resident population of macrophages, T-/B-cells, mast cells and dendritic cells that carry out important surveillance and innate immune functions. Of particular interest is the accumulating evidence that the adventitia is as a stem/progenitor cell niche of the vessel wall of both arteries and veins [74-76]. Progenitor cells are present in vessels of both human and murine origin, and they are described to contribute to the formation of atherosclerotic plaques [75, 77, 78] in in vivo models [79]. For example, Hu et al. [75] demonstrated that Sca-1^+ cells can differentiate into SMCs and contribute to the development of neointima formation. Moreover, perivascular fibroblasts may also be involved in matrix deposition as these cells may exhibit secretive phenotype of smooth muscle cells (myofibroblast) while migrating from the adventitia towards the media [57]. Adherence molecule E-selectin has been shown to be induced in the post-injury adventitial layer, and furthermore, mediates subsequent leucocyte infiltration [59]. Several processes and pro-inflammatory factors have been proposed to act locally to contribute to the activation of the adventitial compartment, ranging from enhanced growth factor activity [80] and increased extracellular matrix synthesis [81] to generation of reactive oxygen species [82]. Considering these evidences, the adventitia is no longer regarded as a relatively ‘inert’ layer providing only supportive connective tissue, but it is a complex community of interactive cells that convey pathologic stimuli.

2. The Biomechanics Experienced by Saphenous Vein Grafts

Mechanical stimulation is an integral component of the cardiovascular developmental process. For example, the beginning of pulsatile flow in the

primary vascular system is a trigger of vascular and cardiac development, likely due to biomechanical effects on differentiation of cardiac and vascular progenitors.

In VGD a crucial component contributing to the pathology is the change in the pressure load and shear stress consequent to arterialization, these biomechanical changes are believed to activate pathways causing IH. In fact, in normal conditions SVs are subjected to quasi-steady flow patterns and are exposed to very low shear stresses (0.1-0.6 Pa) and pressure loads (5-10 mmHg) [58]. By contrast, after CABG, SV segments undergo fast pulsatile flow and the new hemodynamic stimuli are similar to those experienced by coronary arteries: mean flow rate up to 250 ml/min, a high wall shear stress in the range of 0.75-2.25 Pa, a systolic/diastolic pressure of approximately 120/80 mmHg with a circumferential strain of 10-15%. These altered hemodynamic parameters are supposed to cause adaptive remodeling in the SV wall, potentially leading to stimulate vein SMCs proliferation and progressive bypass occlusion.

Moreover, after encountering arterial flow patterns increased levels of intracellular adhesion molecule-1, vascular cell adhesion molecule-1, and monocyte chemotactic protein-1 facilitate leukocyte-endothelial interactions so that leukocyte infiltration of the lesions will ensue [61].

In some experimental models that supported the vein graft with a vascular external sheath, graft failure was prevented due to reduced direct wall stretch force [62, 63]. Moreover, it has been demonstrated that IH does not occur in vein-to-vein isografts. Thus, it can be stated that pathologic changes seen in SVG in the arterial circulation might be caused by hemodynamic and physiochemical changes [61].

2.1. Approaches to Study Vein Graft Failure

The common approach to study VGD takes advantage of the animal model of superior vena cava transplantation in carotid artery.

Beside the in vivo studies, another way to investigate VGD is adopting the ex vivo approach, whereby tailored culture systems able to stimulate vascular tissues with different forces or biochemical factors are used. This approach allow dissecting the contribution of different biochemical/biophysical factors to the onset/progression/establishment of

VGD. Moreover, it permits to study the pathology on animal samples or directly on human samples, a great advantage in understanding mechanisms underlying human vein graft disease.

Several attempts have been made at mimicking the arterial conditions and characterize molecular pathways implicated in SVs arterialization.
To achieve this goal, ex vivo vessel perfusion culture systems (EVPCS) have been developed. In these systems, the survival of vessel segments is ensured by immersion into culture media, and vessel mechanical stimulation is performed by an appropriate arterial-like perfusion of the vessel lumen.
These systems allowed culturing SV segments for different periods; however, they had the limitation of not including a pressure control, which is crucial to mimic the pulsatile arterial-like flow, recognized as one of the causes of vessel patency reduction. Therefore, these systems were only able to elicit biological responses associated to vessel perfusion with constant flows, and, paradoxically, demonstrated the role of laminar shear stress on IH inhibition [64, 65].

A significant advancement toward the development of EVPCSs as tools to mimic SV arterialization has been the inclusion of controllers able to elevate the SV intraluminal pressure. The most advanced perfusion system devised so far was the platform devised by Dummler and colleagues [66]. These Authors developed an EVPCS to perform pulsatile ex vivo stimulation of SVs under venous (flow rate of 5 ml/min, pressure of 10 mmHg) or arterial (flow rate of 50 ml/min, pressure of 100 mmHg) conditions. The biological results obtained using this device showed a relatively rapid occurrence of morphological changes in the vein structure, especially in the media and in the intima layers. These morphological changes were also associated with an increase in the expression of matrix metalloprotease-2 (MMP-2).
Finally, ex vivo stimulation of porcine SVs with different flow rates (5-85 ml/min), shear stress (0.26-5.6 Pa) and pressure (25-90 mmHg) amounts was performed by Clerin and colleagues [67, 68]. Interestingly, in these reports SVs were perfused with culture medium added with Dextran in order to mimic blood viscosity (~4 cP). The main result of these studies showed that

increases in laminar shear stress neutralized intimal thickening, while ramped perfusion pressures induced IH in a dose-dependent manner.
The latest development in EVPCS has been the design of systems allowing the stimulation of vessel segments with sine-like pressure patterns at defined frequencies. In a first example, Saucy and colleagues [69] investigated the impact of high flow pulsatile perfusion (high shear stress in the range of 0.9-1.5 Pa obtained by applying a flow rate of 120±15 ml/min, a pulse rate of 60 pulse/min, and a systolic/diastolic pressure of 80±10/40±10 mmHg) on human SV segments for 14 days. By this, the authors were able to link expression of extracellular matrix remodeling enzymes and a biomechanical stimulus [70], they observed elevation of cellular proliferation in the vein wall as early as at 4 days after the beginning of mechanical conditioning.

In this framework, it might be relevant to design new engineered platforms containing minimized volumes, or system that allow the outer and the inner vein layers to be exposed to different conditions (drugs, hematochemical environment). In this way, for example, the effect of novel therapeutic agents such as gene-transferring vectors, small interfering RNAs (siRNAs) or even antagomirs [71, 72] might be studied for their inhibitory effects on IH. Another advantage of using systems constituted by two chambers, might be the option to add in the inner and/or the outer stimulation circuit living cells and assess their contribution to the IH prevention/progression. This may also open the way to novel tissue engineering approaches using circulating EPCs to perform grafts “pre-endothelialization” [73].

3. Scope of the thesis

Saphenous vein (SV) graft disease represents an unresolved problem in coronary artery bypass grafting (CABG). After CABG, autologous SVs are transposed in arterial position to restore the adequate blood supply to the ischemic myocardium. Beside acute failing of vein graft, a progressive remodeling of the SV wall occurs, leading to thickening of vein wall and subsequent occlusion of the lumen, a process termed 'intima hyperplasia' (IH). IH is mainly due to uncontrolled proliferation of SMCs resident in the vein wall that switch their phenotype from contractile to secretive, starting the deposition of extracellular matrix. During VGD pathogenesis and progression numerous and complex mechanisms influence the course of this disease, for example altered hemodynamic environment, inflammation, resident cells phenotype switching, activation of pathologic molecular activators. While animal transplantation and in vitro models have clarified the role of some remodeling factors, the pathology of human SV is far from being completely understood. The investigation of IH progression is a primary end-point toward the generation of therapies and tools to create occlusion-free vessels that may be used as 'life-long' grafts. The new hemodynamic forces experienced in coronary position, are pathologic stimuli that constantly act on vein grafts contributing to IH; these are unavoidable forces present during the lifetime of the graft.

The aim of this doctoral thesis is to assess the cellular and molecular effects that pulsatile arterial pressure load elicit on the early events underlying vein graft disease. To achieve this goal an ex vivo approach by which an experimental campaign of biomechanical conditioning on human SV segments was carried out. This thesis takes advantages from the design of an ex vivo vein culture system (EVCS) (described in Chapter II) capable of replicating the altered pressure pattern experienced by SV after CABG (80-120mmHg) and the physiologic venous-like perfusion (3ml/min, 5mmHg). The design and prototyping of the ex vivo platform were performed at the Laboratory of Experimental Micro and Biofluid-dynamics (μBS Lab) of the Dipartimento di Elettronica, Informazione e Bioingegneria of Politecnico di Milano. Chapter II illustrates not only the design of EVCS, but also its

biological validation describing the main morphological changes caused in vein segments undergoing arterial-like pressure stimulation. Chapter III describes an advanced study of cellular and molecular mechanisms activated by CABG-like pressure stimulation that might be involved in vein graft disease.

This project is part of a wider study with the aim to find out one or more treatments that can avoid the development of intima hyperplasia in SV grafts. These include pharmacologic or, more in general, preconditioning treatments of SVs segments before their implant as coronary grafts. In this view, the identification of molecular targets pivotal for the onset/early progression of intimal hyperplasia in SV grafts is of primary importance.

4. References

1. Bourassa, M.G., et al., *Long-term fate of bypass grafts: the Coronary Artery Surgery Study (CASS) and Montreal Heart Institute experiences.* Circulation, 1985. **72**(6 Pt 2): p. V71-8.
2. Dougenis, D. and A.H. Brown, *Long-term results of reoperations for recurrent angina with internal mammary artery versus saphenous vein grafts.* Heart, 1998. **80**(1): p. 9-13.
3. Foo, S.S., et al., *Ephrin-B2 controls cell motility and adhesion during blood-vessel-wall assembly*. Cell, 2006. **124**(1): p. 161-73.
4. Kullander, K. and R. Klein, *Mechanisms and functions of Eph and ephrin signalling.* Nat Rev Mol Cell Biol, 2002. **3**(7): p. 475-86.
5. Kudo, F.A., et al., *Venous identity is lost but arterial identity is not gained during vein graft adaptation.* Arterioscler Thromb Vasc Biol, 2007. **27**(7): p. 1562-71.
6. Mitra, A.K., D.M. Gangahar, and D.K. Agrawal, *Cellular, molecular and immunological mechanisms in the pathophysiology of vein graft intimal hyperplasia.* Immunol Cell Biol, 2006. **84**(2): p. 115-24.
7. Palmer, R.M., A.G. Ferrige, and S. Moncada, *Nitric oxide release accounts for the biological activity of endothelium-derived relaxing factor.* Nature, 1987. **327**(6122): p. 524-6.
8. Furchgott, R.F., *Endothelium-derived relaxing factor: discovery, early studies, and identification as nitric oxide.* Biosci Rep, 1999. **19**(4): p. 235-51.
9. Radomski, M.W., R.M. Palmer, and S. Moncada, *The anti-aggregating properties of vascular endothelium: interactions between prostacyclin and nitric oxide.* Br J Pharmacol, 1987. **92**(3): p. 639-46.
10. Radomski, M.W., R.M. Palmer, and S. Moncada, *Endogenous nitric oxide inhibits human platelet adhesion to vascular endothelium.* Lancet, 1987. **2**(8567): p. 1057-8.
11. Bath, P.M., et al., *Nitric oxide and prostacyclin. Divergence of inhibitory effects on monocyte chemotaxis and adhesion to endothelium in vitro.* Arterioscler Thromb, 1991. **11**(2): p. 254-60.
12. Joannides, R., et al., *Nitric oxide is responsible for flow-dependent dilatation of human peripheral conduit arteries in vivo.* Circulation, 1995. **91**(5): p. 1314-9.
13. Reilly, C.F. and R.C. McFall, *Platelet-derived growth factor and transforming growth factor-beta regulate plasminogen activator inhibitor-1 synthesis in vascular smooth muscle cells.* J Biol Chem, 1991. **266**(15): p. 9419-27.
14. Snow, A.D., et al., *Heparin modulates the composition of the extracellular matrix domain surrounding arterial smooth muscle cells.* Am J Pathol, 1990. **137**(2): p. 313-30.
15. Clowes, A.W. and M.J. Karnowsky, *Suppression by heparin of smooth muscle cell proliferation in injured arteries.* Nature, 1977. **265**(5595): p. 625-6.
16. Bryan, A.J. and G.D. Angelini, *The biology of saphenous vein graft occlusion: etiology and strategies for prevention.* Curr Opin Cardiol, 1994. **9**(6): p. 641-9.
17. Davies, M.G. and P.O. Hagen, *Pathophysiology of vein graft failure: a review.* Eur J Vasc Endovasc Surg, 1995. **9**(1): p. 7-18.
18. Thiene, G., et al., *Histological survey of the saphenous vein before its use as autologous aortocoronary bypass graft.* Thorax, 1980. **35**(7): p. 519-22.
19. de Graaf, R., et al., *N-acetylcysteine prevents neointima formation in experimental venous bypass grafts.* Br J Surg, 2009. **96**(8): p. 941-50.
20. Angelini, G.D., et al., *Nature and pressure dependence of damage induced by distension of human saphenous vein coronary artery bypass grafts.* Cardiovasc Res, 1987. **21**(12): p. 902-7.
21. Bush, H.L., Jr., et al., *The natural history of endothelial structure and function in arterialized vein grafts.* J Vasc Surg, 1986. **3**(2): p. 204-15.
22. Ohta, O. and A. Kusaba, *Development of vasa vasorum in the arterially implanted autovein bypass graft and its anastomosis in the dog.* Int Angiol, 1997. **16**(3): p. 197-203.
23. Shi, Y., et al., *Remodeling of autologous saphenous vein grafts. The role of perivascular myofibroblasts.* Circulation, 1997. **95**(12): p. 2684-93.
24. Panetta, T.F., et al., *Unsuspected preexisting saphenous vein disease: an unrecognized cause of vein bypass failure.* J Vasc Surg, 1992. **15**(1): p. 102-10; discussion 110-2.

25. He, G.W., *Vascular endothelial function related to cardiac surgery.* Asian Cardiovasc Thorac Ann, 2004. **12**(1): p. 1-2.
26. Ahmed, S.R., et al., *Human saphenous vein and coronary bypass surgery: ultrastructural aspects of conventional and "no-touch" vein graft preparations.* Histol Histopathol, 2004. **19**(2): p. 421-33.
27. Bourassa, M.G., et al., *Changes in grafts and coronary arteries after saphenous vein aortocoronary bypass surgery: results at repeat angiography.* Circulation, 1982. **65**(7 Pt 2): p. 90-7.
28. Rosenfeldt, F.L., et al., *Pharmacology of coronary artery bypass grafts.* Ann Thorac Surg, 1999. **67**(3): p. 878-88.
29. Lee, M.S., et al., *Molecular and cellular basis of restenosis after percutaneous coronary intervention: the intertwining roles of platelets, leukocytes, and the coagulation-fibrinolysis system.* J Pathol, 2004. **203**(4): p. 861-70.
30. Davies, M.G. and P.O. Hagen, *Pathobiology of intimal hyperplasia.* Br J Surg, 1994. **81**(9): p. 1254-69.
31. Ishiwata, S., et al., *Postangioplasty restenosis: platelet activation and the coagulation-fibrinolysis system as possible factors in the pathogenesis of restenosis.* Am Heart J, 1997. **133**(4): p. 387-92.
32. Knatterud, G.L., et al., *Long-term effects on clinical outcomes of aggressive lowering of low-density lipoprotein cholesterol levels and low-dose anticoagulation in the post coronary artery bypass graft trial. Post CABG Investigators.* Circulation, 2000. **102**(2): p. 157-65.
33. Huynh, T., et al., *Aspirin, warfarin, or the combination for secondary prevention of coronary events in patients with acute coronary syndromes and prior coronary artery bypass surgery.* Circulation, 2001. **103**(25): p. 3069-74.
34. Motwani, J.G. and E.J. Topol, *Aortocoronary saphenous vein graft disease: pathogenesis, predisposition, and prevention.* Circulation, 1998. **97**(9): p. 916-31.
35. Schepers, A., et al., *Anti-MCP-1 gene therapy inhibits vascular smooth muscle cells proliferation and attenuates vein graft thickening both in vitro and in vivo.* Arterioscler Thromb Vasc Biol, 2006. **26**(9): p. 2063-9.
36. Diacovo, T.G., et al., *A functional integrin ligand on the surface of platelets: intercellular adhesion molecule-2.* J Clin Invest, 1994. **94**(3): p. 1243-51.
37. Zou, Y., et al., *Reduced neointima hyperplasia of vein bypass grafts in intercellular adhesion molecule-1-deficient mice.* Circ Res, 2000. **86**(4): p. 434-40.
38. Diacovo, T.G., et al., *Neutrophil rolling, arrest, and transmigration across activated, surface-adherent platelets via sequential action of P-selectin and the beta 2-integrin CD11b/CD18.* Blood, 1996. **88**(1): p. 146-57.
39. Simon, D.I., et al., *Platelet glycoprotein ibalpha is a counterreceptor for the leukocyte integrin Mac-1 (CD11b/CD18).* J Exp Med, 2000. **192**(2): p. 193-204.
40. Wolff, R.A., et al., *Macrophage depletion reduces monocyte chemotactic protein-1 and transforming growth factor-beta1 in healing rat vein grafts.* J Vasc Surg, 2004. **39**(4): p. 878-88.
41. Zhang, L., et al., *Graft-extrinsic cells predominate in vein graft arterialization.* Arterioscler Thromb Vasc Biol, 2004. **24**(3): p. 470-6.
42. Cayci, C., et al., *Naringenin inhibits neointimal hyperplasia following arterial reconstruction with interpositional vein graft.* Ann Plast Surg, 2010. **64**(1): p. 105-13.
43. Adkins, J.R., et al., *Rapamycin inhibits release of tumor necrosis factor-alpha from human vascular smooth muscle cells.* Am Surg, 2004. **70**(5): p. 384-7; discussion 387-8.
44. Schachner, T., et al., *Rapamycin treatment is associated with an increased apoptosis rate in experimental vein grafts.* Eur J Cardiothorac Surg, 2005. **27**(2): p. 302-6.
45. Bretschneider, E., et al., *Factor Xa acts as a PDGF-independent mitogen in human vascular smooth muscle cells.* Thromb Haemost, 2000. **84**(3): p. 499-505.
46. Mackman, N., *Role of tissue factor in hemostasis, thrombosis, and vascular development.* Arterioscler Thromb Vasc Biol, 2004. **24**(6): p. 1015-22.
47. Giesen, P.L., et al., *Blood-borne tissue factor: another view of thrombosis.* Proc Natl Acad Sci U S A, 1999. **96**(5): p. 2311-5.
48. Peykar, S., et al., *Saphenous vein graft disease.* Minerva Cardioangiol, 2004. **52**(5): p. 379-90.
49. Barboriak, J.J., et al., *Pathologic findings in the aortocoronary vein grafts. A scanning electron microscope study.* Atherosclerosis, 1978. **29**(1): p. 69-80.

50. Domanski, M.J., et al., *Prognostic factors for atherosclerosis progression in saphenous vein grafts: the postcoronary artery bypass graft (Post-CABG) trial. Post-CABG Trial Investigators.* J Am Coll Cardiol, 2000. **36**(6): p. 1877-83.
51. Wainwright, C.L., A.M. Miller, and R.M. Wadsworth, *Inflammation as a key event in the development of neointima following vascular balloon injury.* Clin Exp Pharmacol Physiol, 2001. **28**(11): p. 891-5.
52. Turner, N.A., et al., *Selective gene silencing of either MMP-2 or MMP-9 inhibits invasion of human saphenous vein smooth muscle cells.* Atherosclerosis, 2007. **193**(1): p. 36-43.
53. Ni, J., A. Waldman, and L.M. Khachigian, *c-Jun regulates shear- and injury-inducible Egr-1 expression, vein graft stenosis after autologous end-to-side transplantation in rabbits, and intimal hyperplasia in human saphenous veins.* J Biol Chem, 2010. **285**(6): p. 4038-48.
54. Eefting, D., et al., *In vivo suppression of vein graft disease by nonviral, electroporation-mediated, gene transfer of tissue inhibitor of metalloproteinase-1 linked to the amino terminal fragment of urokinase (TIMP-1.ATF), a cell-surface directed matrix metalloproteinase inhibitor.* J Vasc Surg, 2010. **51**(2): p. 429-37.
55. Thomas, A.C. and A.C. Newby, *Effect of matrix metalloproteinase-9 knockout on vein graft remodelling in mice.* J Vasc Res, 2010. **47**(4): p. 299-308.
56. Kallenbach, K., et al., *Inhibition of smooth muscle cell migration and neointima formation in vein grafts by overexpression of matrix metalloproteinase-3.* J Vasc Surg, 2009. **49**(3): p. 750-8.
57. Shi, Y., et al., *Adventitial myofibroblasts contribute to neointimal formation in injured porcine coronary arteries.* Circulation, 1996. **94**(7): p. 1655-64.
58. Malek, AM., et. al., *Hemodynamic shear stress and its role in atherosclerosis.* JAMA 1999; **282**(21): 2035-42
59. Gotoh, R., et al., *E-selectin blockade decreases adventitial inflammation and attenuates intimal hyperplasia in rat carotid arteries after balloon injury.* Arterioscler Thromb Vasc Biol, 2004. **24**(11): p. 2063-8.
60. Siow, R.C. and A.T. Churchman, *Adventitial growth factor signalling and vascular remodelling: potential of perivascular gene transfer from the outside-in.* Cardiovasc Res, 2007. **75**(4): p. 659-68.
61. Zou, Y., et al., *Mouse model of venous bypass graft arteriosclerosis.* Am J Pathol, 1998. **153**(4): p. 1301-10.
62. Vijayan, V., et al., *External supports and the prevention of neointima formation in vein grafts.* Eur J Vasc Endovasc Surg, 2002. **24**(1): p. 13-22.
63. Jeremy, J.Y., et al., *A bioabsorbable (polyglactin), nonrestrictive, external sheath inhibits porcine saphenous vein graft thickening.* J Thorac Cardiovasc Surg, 2004. **127**(6): p. 1766-72.
64. Porter, K.E., et al., *The development of an in vitro flow model of human saphenous vein graft intimal hyperplasia.* Cardiovasc Res, 1996. **31**(4): p. 607-14.
65. Rey, J., et al., *Comparative assessment of intimal hyperplasia development after 14 days in two different experimental settings: tissue culture versus ex vivo continuous perfusion of human saphenous vein.* J Surg Res, 2004. **121**(1): p. 42-9.
66. Dummler, S., et al., *Pulsatile ex vivo perfusion of human saphenous vein grafts under controlled pressure conditions increases MMP-2 expression.* Biomed Eng Online, 2011. **10**: p. 62.
67. Clerin, V., et al., *Mechanical environment, donor age, and presence of endothelium interact to modulate porcine artery viability ex vivo.* Ann Biomed Eng, 2002. **30**(9): p. 1117-27.
68. Clerin, V., et al., *Tissue engineering of arteries by directed remodeling of intact arterial segments.* Tissue Eng, 2003. **9**(3): p. 461-72.
69. Saucy, F., et al., *Ex vivo pulsatile perfusion of human saphenous veins induces intimal hyperplasia and increased levels of the plasminogen activator inhibitor 1.* Eur Surg Res, 2010. **45**(1): p. 50-9.
70. Voisard, R., et al., *Pulsed perfusion in a venous human organ culture model with a Windkessel function (pulsed perfusion venous HOC-model).* Med Sci Monit, 2010. **16**(11): p. CR523-9.
71. McDonald, R.A., et al., *MicroRNA and vascular remodelling in acute vascular injury and pulmonary vascular remodelling.* Cardiovasc Res, 2012. **93**(4): p. 594-604.
72. Wiedemann, D., et al., *Perivascular administration of drugs and genes as a means of reducing vein graft failure.* Curr Opin Pharmacol, 2012. **12**(2): p. 203-16.

73. Griese, D.P., et al., *Isolation and transplantation of autologous circulating endothelial cells into denuded vessels and prosthetic grafts: implications for cell-based vascular therapy.* Circulation, 2003. **108**(21): p. 2710-5.
74. Campagnolo, P., et al., *Human adult vena saphena contains perivascular progenitor cells endowed with clonogenic and proangiogenic potential.* Circulation, 2010. **121**(15): p. 1735-45.
75. Hu, Y., et al., *Abundant progenitor cells in the adventitia contribute to atherosclerosis of vein grafts in ApoE-deficient mice.* J Clin Invest, 2004. **113**(9): p. 1258-65.
76. Scott, N.A., et al., *Identification of a potential role for the adventitia in vascular lesion formation after balloon overstretch injury of porcine coronary arteries.* Circulation, 1996. **93**(12): p. 2178-87.
77. Shi, Y., et al., *Remodeling of autologous saphenous vein grafts. The role of perivascular myofibroblasts.* Circulation, 1997. **95**(12): p. 2684-93.
78. Shi, Y., et al., *Adventitial myofibroblasts contribute to neointimal formation in injured porcine coronary arteries.* Circulation, 1996. **94**(7): p. 1655-64.
79. Zengin, E., et al., *Vascular wall resident progenitor cells: a source for postnatal vasculogenesis.* Development, 2006. **133**(8): p. 1543-51.
80. Shi, Y., et al., *Transforming growth factor-beta 1 expression and myofibroblast formation during arterial repair.* Arterioscler Thromb Vasc Biol, 1996. **16**(10): p. 1298-305.
81. Shi, Y., et al., *Origin of extracellular matrix synthesis during coronary repair.* Circulation, 1997. **95**(4): p. 997-1006.
82. Rey, F.E. and P.J. Pagano, *The reactive adventitia: fibroblast oxidase in vascular function.* Arterioscler Thromb Vasc Biol, 2002. **22**(12): p. 1962-71.

Chapter II:

A compact and automated *ex vivo* vessel culture system for the pulsatile pressure conditioning of human saphenous veins

Marco Piola[1*], Francesca Prandi[2*], Nina Bono[1], Monica Soncini[1], Eleonora Penza[3], Marco Agrifoglio[4], Gianluca Polvani[4], Maurizio Pesce[2] and Gianfranco Beniamino Fiore[1]

[1] Politecnico di Milano, Dipartimento di Elettronica, Informazione e Bioingengeria, Milano, Italy
[2] Laboratorio di Ingengeria Tissutale Cardiovascolare, Centro Cardiologico Monzino-IRCCS, Milano, Italy
[3] II Divisione di Cardiochirurgia, Centro Cardiologico Monzino-IRCCS, Milano, Italy
[4] Dipartimento di Scienze Cliniche e di Comunità, Università di Milano, Milano, Italy

JOURNAL OF TISSUE ENGINEERING AND REGENERATIVE MEDICINE
J Tissue Eng Regen Med (2013) DOI:10.1002/term.1798

*These authors contributed equally to this study

1. Introduction

Coronary artery bypass grafting (CABG) using autologous vessels is a widely used procedure to recover myocardial perfusion in patients with coronary artery disease (de Waard et al., 2006; Parang and Arora, 2009; Wallitt et al., 2007). The saphenous vein (SV), due to its length and superficial anatomical position, represents a preferred natural bypass conduit, especially when the implantation of multiple bypasses is required (Dashwood and Loesch, 2009; Muto et al., 2010; Severyn et al., 2004; Surowiec et al., 2000). Compared with artery-made bypasses (radial and mammary arteries), SV grafts show lower long-term patency; in fact, approximately 15–30% of vein grafts fail during the first year and>50% patients require re-intervention within 10years after implantation (Goldman et al., 2004; Tsui and Dashwood, 2002). The major cause of SV graft failure is an over-proliferation of smooth muscle cells (SMCs) into the vessel intima layer. This process, named 'intimal hyperplasia' (IH), can be detected between 1 month and 1year after graft implantation (Lemson et al., 2000; Motwani and Topol, 1998). However, the beginning of the pathology occurs at much earlier stages after implantation (1week), with the activation of biomechanical- and inflammatory-driven cascades priming vessel remodeling (Mitra et al., 2006; Muto et al., 2010). The new hemodynamic conditions experienced by the vein after implantation in an arterial position are postulated to be an important cause of SV remodeling. In particular, in the coronary artery, the blood flow is characterized by a high pulsatile pressure (80–120mmHg) and a pulsatile flow (mean flow rate of 250ml/min), which results in an elevated shear stress (1–7 Pa) (Bouten et al., 2011; Dummler et al., 2011). Such forces may have antagonistic effects on disease progression. Indeed, elevated shear stress may have an atheroprotective role, due to hemodynamic related increase of nitric oxide (NO) release by endothelial cells, while a non-physiological mechanical loading of the vein wall may have a pro-pathological effect, due to mechanical ruptures in the endothelial layer and abnormal strain of SMC sheets (John, 2009). Various animal models have been devised to address the pathologic evolution of the arterialized veins. These studies have highlighted the relevance of different cell types and signal transduction pathways involved in the initiation of phenomena leading to IH (Hoglund et al., 2010; Torsney et al., 2005). Despite these approaches, however, the establishment of IH in human

arterialized vein is still far from being understood, thus posing the need for novel experimental models to be set up. in order to: (a) tightly reproduce the altered hemodynamic conditions, especially the rise in wall strain; (b) obtain ex vivo arterialized SV segments for investigating the mechanobiological basis of the early events leading to IH at a global molecular level ;and (c) in perspective, attempt therapeutic strategies by pharmacological conditioning of the dynamically cultured vein segments. As we have discussed recently, various devices, tailored to perform ex vivo culture of human SVs for 4–14 days and under dynamic conditions, have been devised (Piola et al., 2012). In this manuscript we propose the design of a compact and automated ex vivo vessel culture system (EVCS) able to artificially produce the effects of arterial pressure-related cyclic wall distention. It is one of the major biomechanical causes of IH in venous CABGs, together with the pulsatile wall shear stress (Anwar et al., 2012; Berceli et al., 1990; John, 2009; Muto et al., 2010; Owens, 2010; Stigler et al., 2012). This aim is achieved by the development and functional assessment of a low-volume, reliable and user-friendly device, capable of automatically replicating the pulsatile pressure patterns of the physiological coronary environment. In perspective, the present EVCS could be used as tool to carry out molecular and cellular studies in order to better understand the impact of modified hemodynamic conditions on in vivo SV remodeling.

2. Materials and methods

2.1. Design of the EVCS

2.1.1. Design specification

The design of the EVCS took into account the general specifications of a bioreactor for tissue-engineering applications (Martin et al., 2004), with particular emphasis on the ease of assembly under a laminar flow hood and the safety of use in a cell culture laboratory. Specifically, the following basic requirements were addressed:

(a) biocompatibility of materials;

(b) transparency, to ensure visual inspection for air bubble and/or medium color changes;

(c) compatibility with sterilization processes, e.g. via autoclaving and/or ethylene oxide (EtO);
(d) minimization of priming volume, in order to limit the cost of soluble culture medium compounds; and finally
(e) ease of vessel accommodation and handling during the EVCS assembly.

2.1.2. Architecture of the ex vivo vessel culture system

The EVCS is designed to apply a CABG-like pressure stimulation (CABG-PS), i.e. a pulsed pressure oscillating between a diastolic minimum and a systolic maximum (e.g. 80–120mmHg), or a steady flow perfusion, i.e. a physiological venous perfusion condition (VP; e.g. 5mmHg) within a controlled and strictly reproducible mechanical environment. A schematic representation of the system's layout is shown in Figure 1C. During culture, SV grafts are hosted in a culture chamber accommodated inside an incubator. The culture chamber is connected to a hydraulic circuit and actuators (pump and solenoid pinch-valve) to apply pressure stimulation to the human vessels or to allow the medium to recirculate within the vessel. The hydraulic actuators are managed by a programmable monitoring and control (M/C) system, which operates via a pressure-based feedback loop.

2.1.3. SV culture chamber

The culture chamber (Figure 1A) includes a commercial reservoir and a purpose-developed vessel housing, which is integrated with the reservoir cap. All the culture chamber parts were built in-house. All the utilized materials are suitable for EtO sterilization. The vessel housing allows hosting SV samples up to 5.5cm in length. The hosted vessel segment is cannulated at both ends and secured using an extensible vessel loop (Esafarma Srl, Italy) as an elastic tourniquet. A standard 50ml Falcon tube acts as a medium reservoir. Five ports through the cap ensure the chamber's connection to the outside. Two ports ensure injection/ removal of the culture medium to/from the vessel (Figure 1A, ports a and b). Two other ports provide connections for recirculation of the reservoir medium, i.e. the medium external to the hosted SV (Figure 1A, ports c and d).

2.1.4. The hydraulic circuit

The hydraulic circuit consists of silicone tubing (Platinum Cured, Cole Parmer, IL, USA) and PP-based pump tubing (PharMed BPT®, Carlo Erba Reagenti, Italy). PP Luer connectors (Cole Parmer) are used to guarantee leak-free connections and facilitate circuit assembly under a laminar flow hood.

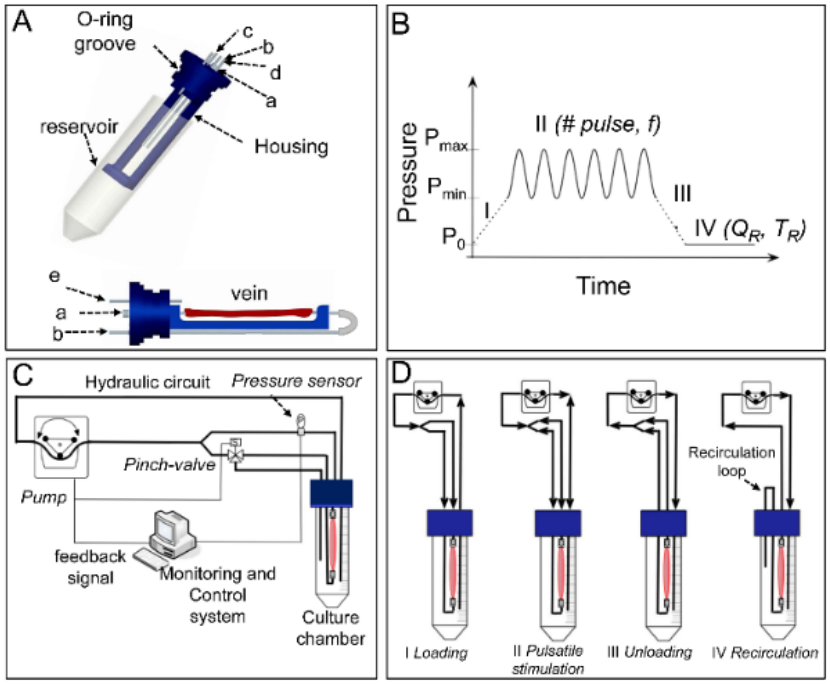

Figure 1. Design of the EVCS. (A) Three-dimensional (3D) CAD model of the SV culture chamber. The chamber consists of the SV housing inserted into a 50 ml Falcon tube, which acts as a reservoir: a and b, ports for the vessel connection sites; c and d, ports for connecting the culture chamber to the hydraulic circuit; e, port for the HEPA filter. (B) Schematic diagram of the CABG-PS program. The CABG-PS consists of: I, a loading phase up to the lower limit of a predefined pressure range; II, pulsatile stimulation in a predefined pressure range; III, an unloading phase; and IV, a recirculation phase. (C) Layout of the EVCS: thick lines, the hydraulic circuit; thin lines, the monitoring and control (M/C) signals. In particular, the M/C system manages the hydraulic actuators (a pump and a solenoid pinch-valve) via a pressure-based signal registered by the pressure sensor. (D) Simplified layout of the flow paths within the EVCS during the CABG-PS cycle. During pulsatile stimulation the medium is forced into and out of the sample through both ends

2.1.5. Monitoring and control system

The M/C system is able to automatically apply the CABG-PS to the SV segments or the SV perfusion by automated control of a peristaltic pump (Watson Marlow 323D, 314D pumping head, UK) and a solenoid pinch-valve (S305-09, SIRAI®, Italy) (Fig. 1C). The solenoid pinch-valve enables switching between the vessel stimulation loop and the recirculation loop (Fig. 1D). The pressure sensor Press-S-000 (PendoTECH, USA) provides the intraluminal pressure feedback signal to the software (Fig. 1C).

2.2. Functional experiments for testing the performance of the EVCS

2.2.1. SV sample preparation

The use of human SV segments was authorized by the local ethical committee with the approval of informed consent. SV segments were obtained from the Department of Cardiovascular Surgery of the Centro Cardiologico Monzino. Briefly, surplus segments of SV were obtained from 19 patients undergoing CABG surgery (mean age 66.7±7.4). The SVs were immediately stored at 4°C in Dulbecco's modified Eagle's medium (DMEM) supplemented with 10% fetal bovine serum (FBS), 1% L-glutamine and 1% penicillin–streptomycin.

2.2.2. Pressure–volume measurements of SV segments

The pressure–volume relationship of human SV segments was obtained in order to dimension the fluid volume that the pump has to process for obtaining the desired pressure increments within the vessel. To this end, a custom-made system was developed to measure the pressure–volume relationship during SV filling. A schematic diagram of the custom-made system is reported in Figure 2A. For each SV specimen (n=6), the inner diameter (D_i) was measured using a caliper. Then, each SV segment was mounted in the custom-made system and pre-tensioned by imposing a 10% axial strain, corresponding to a length named $l_{10\%}$. Table 1 reports the geometrical characteristics (D_i and $l_{10\%}$) of the SV and the volume at zero pressure (V_0), calculated as the volume of a straight cylinder of diameter equal to D_i and length equal to $l_{10\%}$. SV segments were preconditioned by imposing five cycles of loading (0–120mmHg) and unloading (120–

0mmHg), as described in the literature (Costantino et al., 2004). Thereafter, the vessel lumen was exposed to incremental pressure (0–120mmHg; step 10mmHg) and the associated inner volume increment was measured (ΔV, Figure 2A) using an interposed graduated pipette. For each sample, this procedure was repeated three times. The volume increment was normalized toV_0.

2.2.3. Functional assessment of the EVCS

Preliminary tests were performed using a SV sample, mounted within the EVCS, in order to verify the robustness and the reliability of the system over time. The EVCS was placed in the incubator and the performances were evaluated by changing the pulse frequency and the pressure stimulation range. The tested pulse frequencies were 0.5, 0.75, 1 and 1.2 Hz, while the pressure range was 60–90mmHg (hypotension), 80–120mmHg (normal) and 100–140mmHg (hypertension).

2.2.4. Mechanical conditioning of human SV within the EVCS

Generally, the SV samples were each divided into two segments. One portion was immediately stored and used as control (native segment); the second portion (length>5.5cm) was cultured in the EVCS. SV samples were cultured under CABG-PS conditions (luminal pressure, 80–120mmHg; pulse frequency (f), 0.5Hz, with a stimulation interval (T_s) of 10 min; recirculation flow rate (QR) 1ml/min, with a luminal pressure of 1–2mmHg and recirculation interval (TR) of 2min); or VP conditions (steady flow with luminal pressure, 5mmHg; flow rate, 3ml/min). After the sterilization of the EVCS, SV segments were mounted and then the EVCS was filled with 42 ml DMEM with 10% FBS, 1% L-glutamine and 1% streptomycin–penicillin. Then, the EVCS was kept in the incubator at 37°C and 5% CO_2 for a culture period of 7 days. The culture medium was partially changed at day 3. At the end of the mechanical conditioning period, the SV samples were disassembled, vein ends were discharged (thus avoiding any edge effects induced by the mounting onto rigid connectors) and the central portion of the SV was processed for the following analyses.

2.2.5. Tissue viability evaluation

Rings of cultured and native (positive control) SV samples were stained with methylthiazol tetrazolium (MTT; Sigma-Aldrich), final concentration of 0.5 mg/ml. SV rings were incubated at 37°C for 1h in PBS/MTT solution. As a negative control, a SV ring was fixed with 4% formaldehyde overnight and then incubated with MTT staining. After 1h, pictures were taken using a stereomicroscope (STEMI2000-C,CarlZeiss®,Germany).

2.2.6. Morphological and immunofluorescence assessment of the mechanically conditioned human SV segments

Cultured (n=6 VP and n=6 CABG-PS treated samples) and control (n=11) SV samples were fixed with 4% formaldehyde overnight, paraffin-embedded and cut into 5μm thick sections using a microtome. Sections were stained with Masson's trichrome (Bio-Optica Milano SpA, Italy), according to the manufacturer's protocol. Six slices of each SV sample were observed for qualitative inspection, and digital images were acquired using a light microscope (AxioVision Bio Software, Carl Zeiss, Germany) at a magnification of×10. For immunofluorescence (IF) analysis, three samples for each group (VP, CABG-PS and related controls) were observed. Briefly, 4μm thick sections were obtained from formalin-fixed, paraffin-embedded SV specimens. Antigen retrieval was performed with 10mM Tris–HCL/1mM EDTA for 10min in a microwave. Thereafter the sections were incubated with mouse anti human-αSMA (1:500; Dako), goat anti-human CD31 (1:200; Santa Cruz Biotechnology) and rabbit anti-human vWF (1:200; Dako) to label endothelial cells (ECs). The slides were incubated with AlexaFluor 488 anti-mouse, AlexaFluor 546 anti-goat and AlexaFluor 633 anti-rabbit (1:200; Invitrogen) secondary antibodies, and nuclei were counterstained with DAPI (Vector Laboratories, CA, USA). Finally, digital images were obtained using a multicolor detection protocol in an LSM-710 confocal scanning microscope (Carl Zeiss, Germany).

Sample	D_i [mm]	$l_{10\%}$[mm]	V_0 [ml]
SV01	3.2	59	0.47
SV02	3.1	35	0.26
SV03	3.8	60	0.68
SV04	3.4	35	0.27
SV05	3.2	35	0.28
SV06	3.8	60	0.68
Mean	3.4	46.5	0.44

Table 1. Geometric values of the SV samples (n=6) used for the pressure–volume measurements D_i, inner diameter; $l_{10\%}$, length of the sample hosted within the custom-made device; V_0, calculated as the volume of a straight cylinder of diameter D_i and length $l_{10\%}$.

2.2.7. Morphometric measurements

Morphometric analyses were performed on Masson's trichrome-stained sections in order to measure thickness and luminal perimeter. Thickness measurements were manually processed on digital images taken with AxioVision Bio Software (Carl Zeiss) at ×10 magnification. The inner perimeter was calculated using Image-J software (v. 1.47f-software for Java, National Institutes of Health, USA).

2.3. Statistical analysis

Statistical comparisons were performed using Graph-Pad 5 (Prism) statistical software. All data were initially analysed using the Kolmogorov–Smirnov normality test and then compared using a non-parametric Mann–Whitney test. $p<0.05$ was assumed as statistically significant in all statistical tests.

3. Results

3.1. Pressure–volume measurements of SV segments

Figure 2B reports the pressure–volume relationship obtained by progressively inflating the fluid volume in human SV segments. The results showed an initial rapid volume rise with the first pressure increment step from 0 to 10mmHg (a physiological pressure range for veins), followed by a decreasing slope of the pressure–volume relationship, indicating that a considerable stiffening of the SV tissue progressively occurred when shifting towards the arterial pressure range (Fig 2B). Figure 2C reports the luminal volume increment within the vein after imposing a pressure in the ranges 0–10, 10–80 and 80–120mmHg. According to these results, the mean inflation fluid volume necessary to generate a pressure increment from 80 to 120mmHg was 0.06±0.025ml (Fig 2C). This value was used as rough estimate for selecting the dimensions of the relevant hydraulic components, such as the volume of the compliance chamber and the inner diameter of the pump tubing.

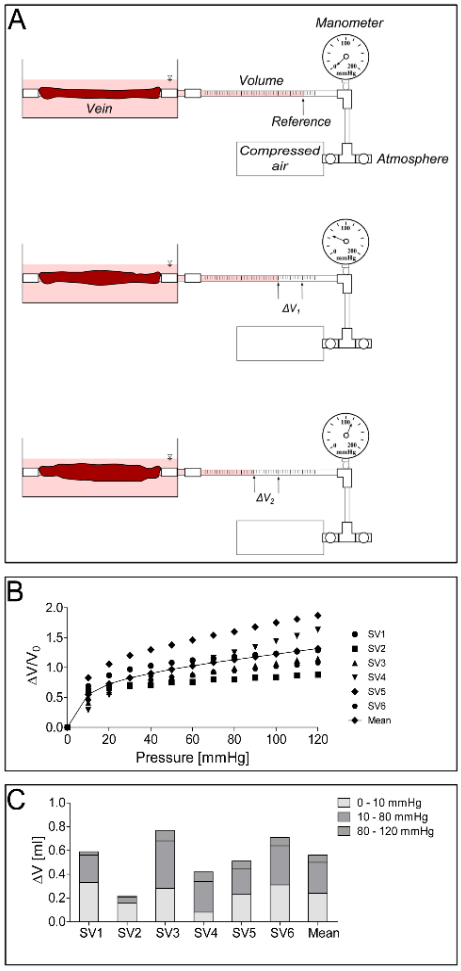

Figure 2. (A) Schematic of the custom-made set-up developed for the compliance measurements. Pressure is measured with a manometer and inner volume increments (ΔV) are measured using a graduated pipette. (B) Pressure vs volume relationship for six human SVs. An initial rapid volume rise at physiological venous pressure range (0–10mmHg) is followed by a decreasing slope at physiological arterial pressure (80–120mmHg). (C) Representative histogram of the inflation volume necessary to generate pressure ranges (0–10, 10–80 and 80–120mmHg) in the vein lumen

3.2. Preliminary functional assessment and setting of EVCS stimulation program

An overview of the EVCS during the assembly phase under a laminar flow hood is shown in Figure 3. Finally, the housing was inserted within the reservoir and connected to the hydraulic circuit (Figure 3E). Once assembled, the EVCS was placed in the incubator and the culture under mechanical conditioning started, imposing either a VP or a CABG-PS condition. The CABG-PS program consisted of a cyclical alternation of a pulsatile stimulation period and a recirculation period. Particularly, the single cycle was composed of four steps (Figure 1B):
(a) the loading step, in which the culture medium was delivered through the vessel until the intraluminal pressure reached a lower pressure limit (P_{min});
(b) the pulsatile stimulation step, during which the vessel was inflated and deflated in order to apply a controlled CABG-PS within the predefined pressure ranges (P_{min}–P_{max}) and for a predefined time and number of pulses/min;

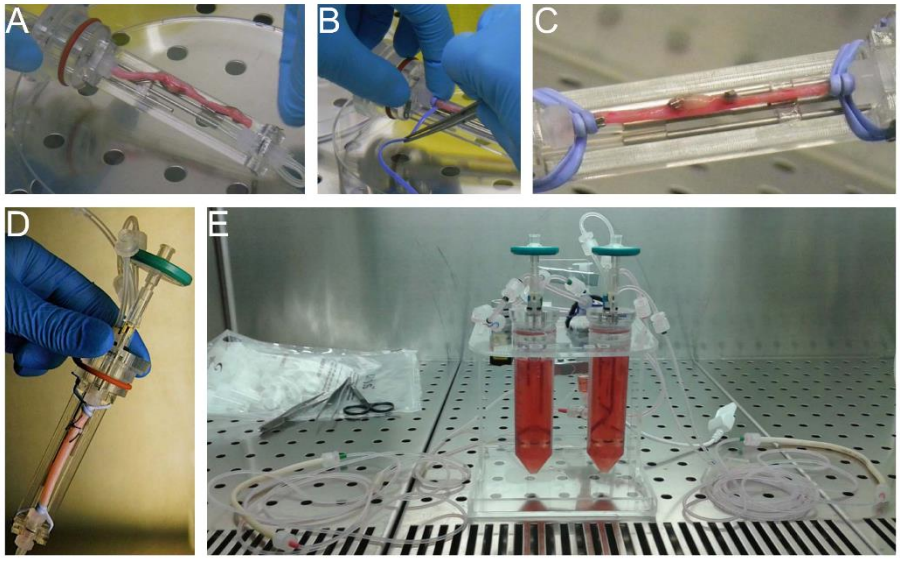

Figure 3. Prototype of the EVCS during the assembly phase. (A) The SV sample is mounted in the housing and (B) secured via vessel loops. (C) After vessel fixing (D) the HEPA filter is mounted onto its port and then the vessel housing is inserted within the reservoir and connected through a silicone O-ring coupling, resulting in a compact culture chamber. (E) The culture chamber is then connected to the hydraulic circuit and the entire system is filled with culture medium.

(c) the unloading step, in which the intra luminal pressure within the vessel was lowered again to zero (P_0) by inverting the medium flow direction;
(d) the recirculation step, characterized by a constant flow rate allowing a metabolic supply to the vessel for a predefined recirculation period.
Figure 4A reports representative screen printouts of the M/C software of the EVCS, showing an example of pressure tracing during the CABG-PS cycle. The outcomes of the functional tests indicated a good reliability of the M/C system. Figure 4B shows the system's response to different pressure conditions reproducing hypertension (100–140mmHg), normal (80–120mmHg) and hypotension (60–90mmHg) conditions; while the system's response to different values of frequency (0.5, 0.75, 1 and 1.2Hz) is shown in Figure 4C. In both configurations, the stimulation pressure tracings were fairly regular, repeatable and compliant to the user's settings. Finally, microbiological tests showed no contamination in the culture medium after 7 days of culture in either tested configuration (silicone vessel or SV sample).

3.3. Validation of the EVCS during culture under mechanical conditioning

The culture of SV segments for 7 days under VP and CABG-PS conditions was finally performed in the EVCS. To assess tissue viability, MTT staining was used (Figure 5). This showed that after 7 days under VP (Figure 5A) or CABG-PS (Figure 5B) conditions the vessel viability was maintained similarly to freshly harvested SV rings, used as positive control (Figure 5C). To assess vessel integrity and structure after VP/CABG-PS periods, Masson's trichrome staining of transverse sections was performed. Results showed a good integrity of the vessel structure with a good preservation of SMCs and the adventitia layers, and without signs of tissue degeneration and swelling (Figure 6). Changes in cellular arrangement were instead observed in the VP (Figure 6B) *vs.* CABG-PS (Figure 6C) segments.

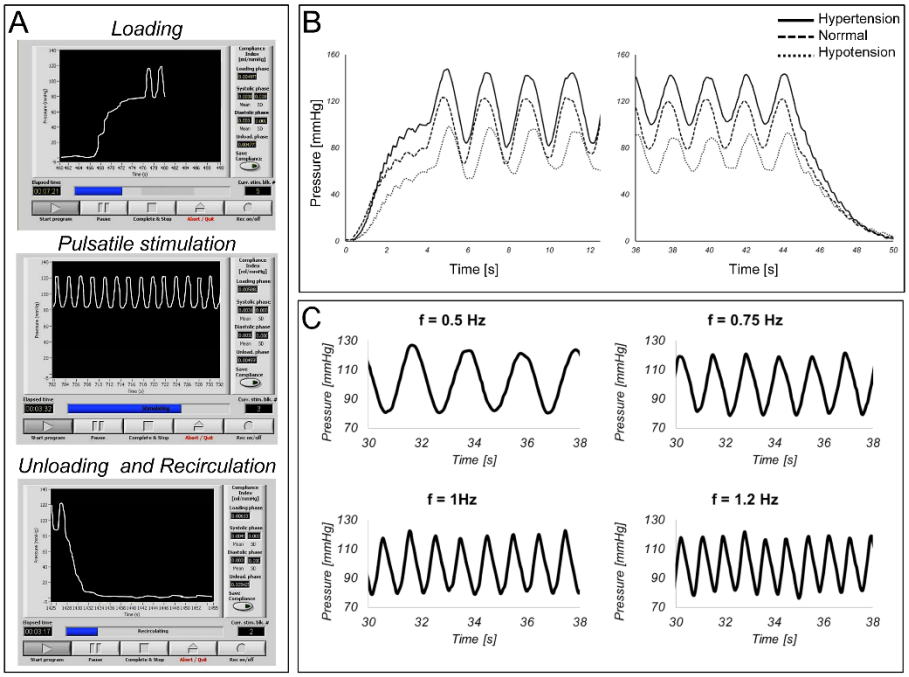

Figure 4. (A) Printout of the resulting pressure tracing during the four steps of the CABG-PS cycle. (B) Pressure tracings of the CABG-PS cycle of a SV segment, obtained by changing the pressure within the ranges 60–90 (hypotension), 80–120 (normal) and 100–140mmHg (hypertension) at a predefined pulse frequency of 0.5Hz. (C) Fragments of the CAGB-PS cycle of a SV segment, obtained by changing the pulse frequency (0.5, 0.75, 1 and 1.2Hz) and applying a normal pressure range to the vessel

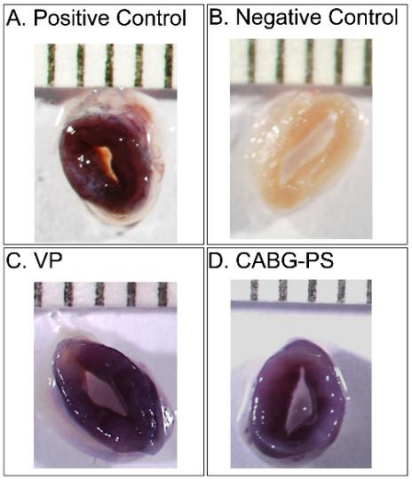

Figure 5. Images of SV rings stained with MTT after 7 days of culture in the EVCS under (A) VP and (B) CABG-PS conditions. Fresh and formaldehyde-fixed tissues were used as positive (C) and negative (D) controls, respectively. The images in the figure are representative of the behavior observed for three VP and three CABG-PS samples and related controls.

In fact, in VP-cultured vessel segments (Figure 6B), the arrangement of medial SMC layers appeared similar to that present in non-cultured vessels (Figure 6A); by contrast, the application of CABG-PS caused an almost complete SMCs disarrangement (Figure 6C). To better evaluate the organization and arrangement of cellular components of the SV following *ex vivo* culture, IF analysis for the SMC marker αSMA was performed (Figure 6, right column). Low-magnification imaging of the vessels confirmed a difference in the medial layer of CABG-PS *vs.* VP vessels, again suggesting a loss in circumferential SMC sheets due to the modified pressure conditions (Figure 6C, right column). Observation of the vessel structure by histochemistry and IF showed that vessels cultured under CABG-PS conditions had a relatively thinner wall and larger lumen than VP or native vessels (Figure 6A–C). To obtain quantitative data, both parameters were evaluated by computer-aided measuring. As shown in Figure 6D, the quantitative evaluation of wall thickness and luminal perimeter revealed major morphometric changes in CABG-PS *vs*. native vessels. Interestingly, veins perfused with a venous pressure did not undergo remodeling, confirming that application of a CABG-PS for 7 days was sufficient to induce structural changes in the SV.

To assess whether the SV endothelium was affected by changes in pressure conditions in CABG-PS vessels an IF analysis for the endothelial markers vWF and CD31 was set up, followed by low- and high- power confocal imaging (Figure 7). Panels A, B and C of Figure 7 show, respectively, low and high power views of the EC layer stained in the same vessels presented in Figure 6A, B and C. While at low magnification the appearance of the endothelial layer appeared similar in the three conditions, the high-power views showed the loss of EC integrity and the partial detachment of the EC layer in CABG-PS *vs.* native and VP-stimulated veins (cf. panels 7C with 7A and 7B).

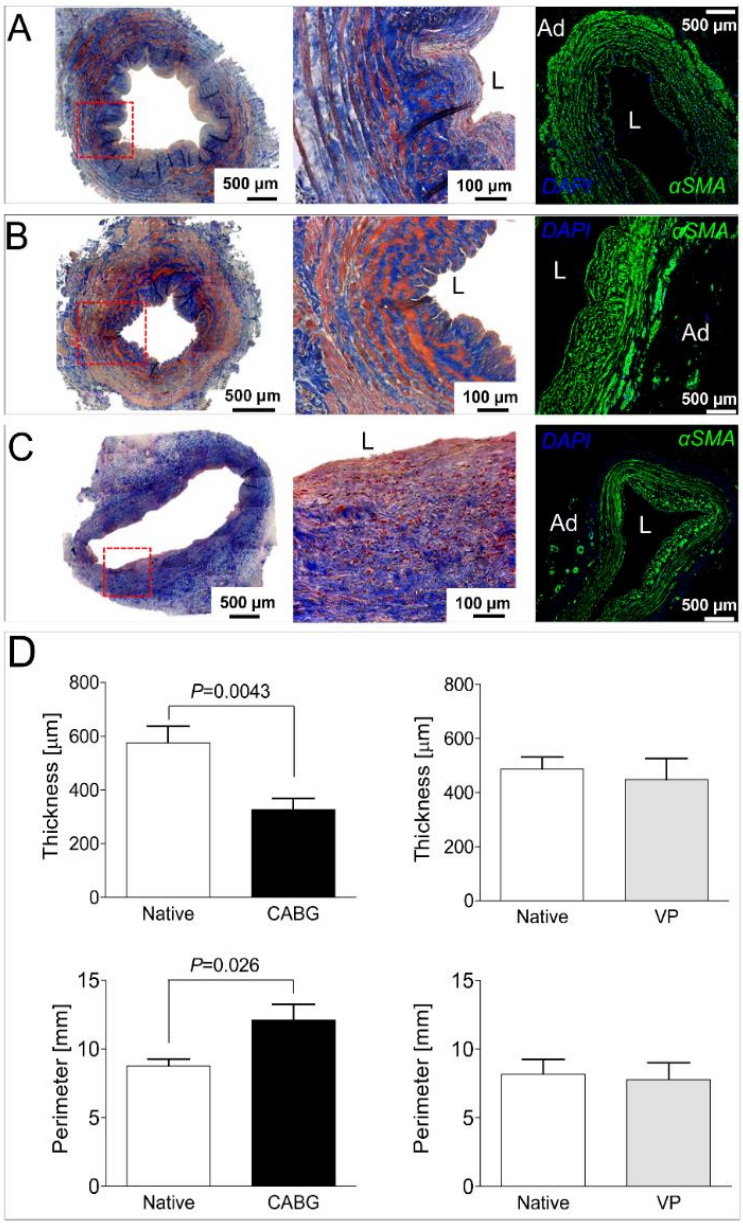

Figure 6. SV tissue sections stained with Masson's trichrome and αSMA/DAPI after 7 days of culture in the EVCS. A major rearrangement of SMCs was observed in CABG-PS *vs.* VP SVs. In each panel, from left to right, low- and high-power views of Masson's trichrome-stained sections and low-power views of αSMA-stained sections are shown in native tissue (A), VP-cultured (B) and CABG-PS (C) SV samples, respectively: L, lumen; Ad, adventitia layer. (D) Thickness and inner perimeter measurements were performed on SV sections stained with Masson's trichrome.

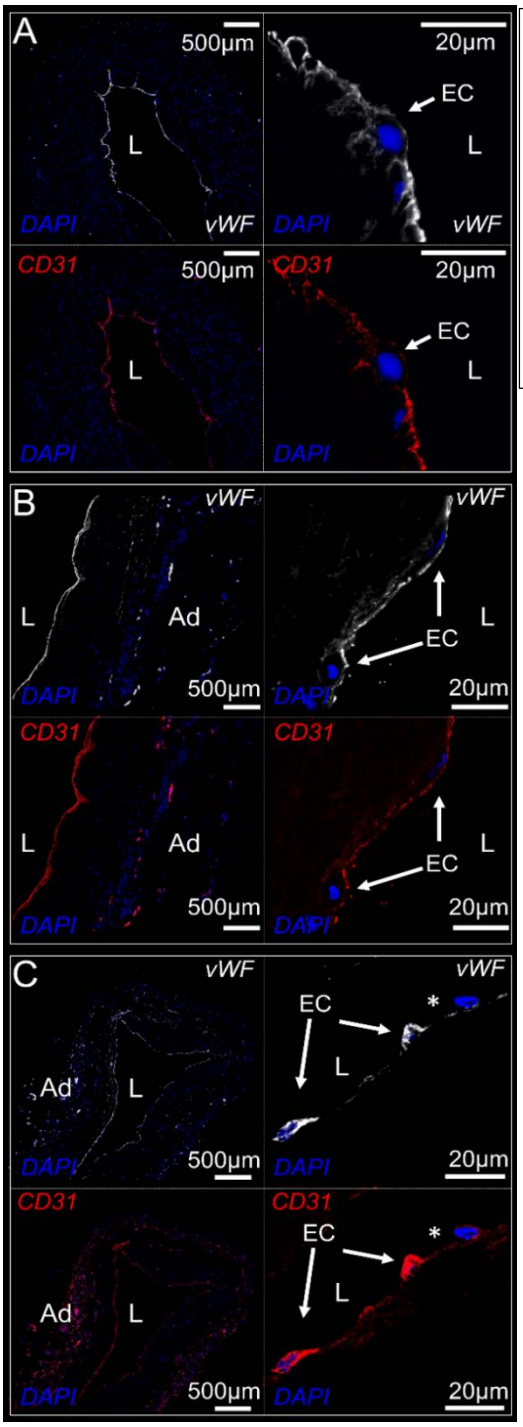

Figure 7. Low- and high-power views of representative IF images in native (A), VP-cultured (B) and CABG-PS (C) SV sample tissue sections stained with vWF- and CD31- specific antibodies: L, vessel lumen; Ad, adventitia layer; arrows, $vWF^{+}/CD31^{+}$ ECs lining the SV lumen. Note the lower immunostaining in the CABG-like (C) *vs.* VP (B)/native (A) vessels and evident endothelial cell rupture, as indicated by partial detachment of the cell from the basal lamina (*)

4. Discussion

In the present contribution, we described the design of a novel and versatile platform to perform dynamic stimulation of SV segments mimicking the physiological pressure patterns of the coronary circulation. This condition is indicated as one of the major insults received by the SV segments following CABG implantation (Anwar et al., 2012; Berceli et al., 1990; John, 2009; Muto et al., 2010; Owens, 2010). Hence, the rationale of its choice as a controlled factor for conditioning SV segments is to enable *ex vivo* campaigns for elucidating the role of a major biomechanical factor in SV arterialization. The EVCS was verified to reliably apply the desired pressure patterns to SV segments and to maintain the viability of the vessels at least for 7 days in a controlled and sterile environment.

4.1. Enhanced versatility and automation of an ECVS for ex vivo vessel conditioning

Regarding the EVCS design, the specifications of easy assembly and handling were satisfied, thanks to the technical solutions adopted. First, the entire system is very compact through the adoption of an integrated medium reservoir, which makes the device easy to use in a standard cell culture incubator. In addition, compactness allowed the overall priming volume to be reduced to 42 ml. Finally, working in vertical conditions facilitates the air debubbling through the HEPA port during the assembly and filling of the EVCS. Compared to other EVCSs reported in literature (Piola et al., 2012), our EVCS is designed to ensure the perfusion of the hosted SV segments or to impose controlled physiological CABG-PS conditions, resulting in a cyclic wall circumferential strain. To this purpose, the EVCS is equipped with dedicated control hardware and software, which, from the user's standpoint, implies interaction with a programmable and user-friendly graphical interface. The strategy we adopted for pressure stimulation consisted of inflating and deflating the SV by forcing small volumes of medium into and out of the vessel through both ends. Thus, a recirculation phase is mandatory in order to re-establish the correct amount of nutrients within the luminal region of the vein. In addition, pulse generation is based on the commands of a robust programmable M/C system, which operates via a pressure-based auto-tuning feedback loop. A main feature of the M/C

system is the possibility to freely set different stimulation parameters, such as pressure range, pulse frequency and number of cycles, in order to properly modulate the stimulation pattern. In this manner, a versatile system is envisaged, with the capability to perform simultaneous stimulation of SV segments under different conditions. Our EVCS suffers from some limitations. The system does not allow for the application of a coronary-mimicking flow through the vessel, hence the shear stress stimulus deriving from the arterial transposition of the vein is not replicated. Specifically, the net flow being approximately zero during the stimulation period, the resulting shear stress experienced by the ECs in the EVCS is negligible with respect to arterial shear stress. On the one hand, this allowed us to selectively study the early remodeling effects caused by wall strain alone as a biomechanical stimulus. The system, however, is amenable to a fully biomimetic upgrade; this will require minimal changes to the culture chamber design, whereas appropriate refinements will be needed for the hydraulic circuit layout and for the M/C system. In addition, the system is not suitable for replicating the artery/vein compliance mismatch, hampering the possibility of studying its contribution to the early remodeling events associated with IH. The pressure–volume relationship of human SVs, obtained experimentally, was used in order to determine the volume of medium to be processed within the vessel to obtain the desired intraluminal pressure oscillation within the CABG-PS range. In addition, the results indicated that the pressure–volume curves were non-linear and revealed a considerable hardening of the SV tissue occurring at arterial pressures. These data fully comply with data reported in the literature (Stooker et al., 2003). It is worth noticing that, as attested in our functionality tests as well as in the subsequent 7-day device-use experience, pulse-generation stability was not affected at all by the strong non-linearity of the treated samples. From a strictly engineering viewpoint, this is an index of the system's robustness as an automated tool for biomechanical SV sample stimulation.

4.2. Validation of the ECVS using human SV tissues reveals profound changes in vessel structure due to arterial-like wall strain

A major interest for vascular biologists consists in the possibility of investigating the specific contribution of hemodynamic forces involved in vessel pathologies. In particular, platforms able to apply arterial-like

pressure patterns to vein segments maybe crucial to resolve the timely issue of graft patency reduction following CABG surgery (Owens, 2010; Piola et al., 2012). Two major biomechanical components are believed to contribute to vein arterialization: flow shear stress, which is increased in CABG due to a raise in flow velocity, and wall stress/tension, which is also increased due to a switch from venous to arterial pressures (John, 2009). Wall strain is involved in the remodeling of the venous wall, causing the reduction of the SV thickness and the mechanical rupture of the endothelial layer and the underlying SMC sheets (John, 2009; Owens, 2010; Saucy et al., 2010). In a wider view of addressing the role of the different mechanical components involved in IH, the approach followed in the present report confirms an important contribution of arterial-like wall strain in SV structural changes. In fact, our data indicated a clear thinning of the SV wall and a marked enlargement of the luminal perimeter, two parameters which have been found to be significantly changed during arterial positioning of vein segments in patients and animal models (Owens, 2010, and references). In addition, we observed a contribution of the CABG-PS condition to determine microscopic ruptures in the endothelial layer and a striking disarray in the SMC layers in the medial tissue, two factors known to predispose the vessel to pathological remodeling (Motwani and Topol, 1998). In summary, the compact and automated EVCS appears to be a well-suited system able to reproduce the wall strain conditions typical of the coronary circulation. The system maintains optimal tissue viability, operates under sterility and performs vessel stimulation in a low-volume culture chamber. For these enhanced design characteristics, this platform is therefore a novel laboratory-orientated tool that will be useful for carrying out *ex vivo* culture campaigns under strictly controlled hemodynamic conditions and dissecting the contribution of different biomechanical factors involved in early IH priming in vein CABGs.

5. References

Anwar MA, Shalhoub J, Lim CS et al. 2012; The effect of pressure-induced mechanical stretch on vascular wall differential gene expression. J Vasc Res 49: 463–478.

Berard X, Déglise S, Alonso F et al. 2013; Role of hemodynamic forces in the ex vivo arterialization of human saphenous veins. J Vasc Surg 57: 1371 –1382.

Berceli SA, Showalter DP, Sheppeck RA et al. 1990; Biomechanics of the venous wall under simulated arterial conditions. J Biomech 23: 985–989.

Bouten CV, Dankers PY, Driessen Mol A et al. 2011; Substrates for cardiovascular tissue engineering. Adv Drug Deliv Rev 63: 221 –241.

Clerin V, Gusic RJ, O'Brien J et al. 2002; Mechanical environment, donor age, and presence of endothelium interact to modulate porcine artery viability ex vivo. Ann Biomed Eng 30: 1117–1127.

Costantino ML, Bagnoli P, Dini G et al. 2004; A numerical and experimental study of compliance and collapsibility of preterm lamb tracheae. J. Biomech. 37: 1837–1847.

Dashwood MR, Loesch A. 2009; The saphenous vein as a bypass conduit: the potential role of vascular nerves in graft performance. Curr Vasc Pharmacol 7: 47 –57.

Dashwood MR, Tsui JC. 2013; 'No-touch' saphenous vein harvesting improves graft performance in patients undergoing coronary artery bypass surgery: a journey from bedside to bench. Vascul Pharmacol 58: 240–250.

De Waard V, Arkenbout EK, Vos Metal.2006; TR3 nuclear orphan receptor prevents cyclic stretch-induced proliferation of venous smooth muscle cells. Am J Pathol 168: 2027–2035.

Dummler S, Eichhorn S, Tesche C et al. 2011; Pulsatile ex vivo perfusion of human saphenous vein grafts under controlled pressure conditions increases MMP-2 expression. BioMed Eng OnLine 10: 62.

Goldman S, Zadina K, Moritz T et al. 2004; Long-term patency of saphenous vein and left internal mammary artery grafts after coronary artery bypass surgery: results from a Department of Veterans Affairs cooperative study. J Am Coll Cardiol 44: 2149–2156.

Gusic RJ, Myung R, Petko M et al. 2005; Shear stress and pressure modulate saphenous vein remodeling ex vivo. J. Biomech. 38: 1760 –1769.

Hoenicka M, Wiedemann L, Puehler T et al. 2010; Effects of shear forces and pressure on blood vessel function and metabolism in a perfusion bioreactor. Ann. Biomed. Eng. 38: 3706–3723.

Hoglund VJ, Dong XR, Majesky MW. 2010; Neointima formation: a local affair. Arterioscler Thromb Vasc Biol 30: 1877–1879.

John LCH. 2009; Biomechanics of coronary artery and bypass graft disease: potential new approaches. Ann Thorac Surg 87: 331–338.

Lemson MS, Tordoir JH, Daemen MJ et al. 2000; Intimal hyperplasia in vascular grafts. Eur J Vasc Endovasc Surg 19: 336–350.

Martin I, Wendt D, Heberer M. 2004; The role of bioreactors in tissue engineering. Trends Biotechnol 22: 80 –86.

Mitra AK, Gangahar DM, Agrawal DK. 2006; Cellular, molecular and immunological mechanisms in the pathophysiology of vein graft intimal hyperplasia. Immunol Cell Biol 84: 115 –124.

Miyakawa AA, Dallan LAO, Lacchini S et al. 2008; Human saphenous vein organ culture under controlled hemodynamic conditions. Clinics 63: 683–688.

Motwani JG, Topol EJ. 1998; Aortocoronary saphenous vein graft disease: pathogenesis, predisposition, and prevention. Circulation 97: 916 –931.

Muto A, Model L, Ziegler K et al. 2010; Mechanisms of vein graft adaptation to the arterial circulation. Circulat J 74: 1501–1512.

Orr DE, Burg KJL. 2008; Design of a modular bioreactor to incorporate both perfusion flow and hydrostatic compression for tissue engineering applications. Ann. Biomed. Eng. 36: 1228–1241.

Owens CD. 2010; Adaptive changes in autogenous vein grafts for arterial reconstruction: clinical implications. J. Vasc. Surg. 51: 736–746.

Parang P, Arora R. 2009; Coronary vein graft disease: pathogenesis and prevention. Can J Cardiol 25: 57 –62.

Piola M, Soncini M, Prandi F et al. 2012; Tools and procedures for ex vivo vein arterialization, preconditioning and tissue engineering: a step forward to translation to combat the consequences of vascular graft remodeling. Recent Pat Cardiovasc Drug Discov 7: 186 –195.

Saucy F, Probst H, Alonso Fet al. 2010; Ex vivo pulsatile perfusion of human saphenous veins induces intimal hyperplasia and increased levels of the plasminogen activator inhibitor 1. Eur Surg Res 45: 50 – 59.

Severyn DA, Muluk SC, Vorp DA. 2004; The influence of hemodynamics and wall bio-mechanics on the thrombogenicity of vein segments perfused in vitro. J Surg Res 121: 31 –37.

Stigler R, Steger C, Schachner T et al. 2012; The impact of distension pressure on acute endothelial cell loss and neointimal proliferation in saphenous vein grafts. Eur J Cardiothorac Surg 42: e74 –79.

Stooker W, Gök M, Sipkema P et al. 2003; Pressure–diameter relationship in the human greater saphenous vein. Ann. Thorac. Surg. 76: 1533–1538.

Surowiec SM, Conklin BS, Li JS et al. 2000; A new perfusion culture system used to study human vein. J. Surg. Res. 88: 34 –41.

Torsney E, Hu Y, Xu Q. 2005; Adventitial progenitor cells contribute to arteriosclerosis. Trends Cardiovasc Med 15: 64–68.

Tsui JC, Dashwood MR. 2002; Recent strategies to reduce vein graft occlusion: a need to limit the effect of vascular damage. Eur. J. Vasc. Endovasc. Surg. 23: 202–208.

Vismara R, Soncini M, Talò G et al. 2009; A bioreactor with compliance monitoring for heart valve grafts. Ann. Biomed. Eng. 38: 100 –108.

Voisard R, Ramiz E, Baur R et al. 2010; Pulsed perfusion in a venous human organ culture model with a Windkessel function (pulsed perfusion venous HOC-model). Med Sci Monit 16: CR523–529.

Wallitt EJ, Jevon M, Hornick PI. 2007; Therapeutics of vein graft intimal hyperplasia: 100years on. Ann. Thorac. Surg. 84: 3

Chapter III:

Mechanical strain reinforces priming of the human saphenous vein bypass stenosis through adventitial vessel growth and progenitor cells activation

Francesca Prandi[1,*], Marco Piola[2,*], Monica Soncini[2], Claudia Colussi[3], Yuri D'alessandra[4], Eleonora Penza[5], Marco Agrifoglio[6], Maria Cristina Vinci[1], Gianluca Polvani[6], Carlo Gaetano[7], Gianfranco Beniamino Fiore[2] and Maurizio Pesce[1]

[1]Laboratorio di Ingegneria Tissutale Cardiovascolare, Centro Cardiologico Monzino-IRCCS, Milan, Italy.

[2]Politecnico di Milano, Dipartimento di Elettronica, Informazione e Bioingegneria, Milan, Italy.

[3]Istituto di Patologia Medica, Università Cattolica del Sacro Cuore, Rome, Italy.

[4]Laboratorio di Immunologia e Genomica Funzionale, Centro Cardiologico Monzino, IRCCS.

[5]II Divisione di Cardiochirurgia, Centro Cardiologico Monzino-IRCCS, Milan Italy.

[6]Dipartimento di Scienze Cliniche e di Comunità, Università di Milano, Italy.

[7]Division of Cardiovascular Epigenetics, Goethe University, Frankfurt-am-Main, Germany.

*These authors contributed equally to this study

The following work is under editorial board for Arteriosclerosis, Thrombosis, and Vascular Biology (ATVB)

1. Introduction

Coronary artery bypass grafting (CABG) is a standard surgical procedure to re-vascularize the chronically ischemic myocardium since '60s (1). Despite the undoubted clinical benefits, patients receiving saphenous vein (SV) bypass undergo mid- and long-term complications due to progressive reduction of bypass patency, in fact patency drops to around 50% at 10 years after implantation (2-4). The choice of vascular conduits derived from arterial sources such as, e.g., the inner mammary or the radial arteries, have significantly alleviated the impact of coronary artery surgery on patients outcome (5, 6). On the other hand, the use of the SV is unavoidable, especially in cases of multi-vessel coronary artery disease, which require multiple conduits to be grafted (7). In these instances, even if "no touch" SV harvesting modalities preserving the vascular integrity have been introduced (5), there is still a high incidence of venous graft bypass failure.
Numerous *in vivo* studies have addressed the pathophysiology of vein graft disease (VGD). These animal models, performed by transplanting autologous vein segments into arterial position (8), have paved the way to *i)* understand the contribution of different cellular types to intima hyperplasia (IH) (9-13), *ii)* assess the phenotypic changes occurring in vein cells during arterialization (14), *iii)* to test intervention strategies with gene transfer or gene modulation approaches (15-17) and, lately, *iv)* to identify novel arterialization-specific molecular pathways based on micro-RNAs-dependent gene expression programs (18, 19).

Vein bypass stenosis is caused by an over-proliferation of smooth muscle cells (SMCs), being recruited to the vessel intimal layer during the early stages after bypass implantation. These cells, switching from a contractile to a migratory/secretory phenotype, progressively accumulate into the intima layer narrowing the lumen. As final effect the stenosis reduces the amount of the blood flow to the downstream myocardial tissue (4, 20). Secondary effects such as bypass atherosclerosis have been also reported (4). A more recent view takes also into account the substantial participation of vein-resident cells with progenitor characteristics. These cells, have been found in animal and human vessels, where they have been classified as multipotent mesenchymal progenitors of pericyte origin (21-28).

An increasing relevance of the altered hemodynamics in venous grafts failure has been hypothesized. This is based on the acknowledgement that the early structural adaptation of the vessel to the arterial flow, as detected by CT-scan- or 3D-Echo-derived imaging data (29, 30), may predict the temporal evolution of the graft patency (31). In addition, the devise of vessel culture systems mimicking the coronary pressure/flow conditions in cultured vessels (32), offers new tools for studying the relationship between the new hemodynamic environment and the pathologic programming occurring in arterialized veins under ex vivo conditions.

In the present contribution, we provide a novel understanding of the VGD biomechanical basis. To this aim we used an *ex vivo* vein culture system (EVCS) allowing to stimulate human SV segments with venous perfusion or arterial-like wall strain (33, 34), and to investigate the effects of vessel arterialization with an analysis of structural, cellular and molecular responses.

2. Materials and methods

2.1 SV segments preparation. The use of human SV segments was approved by the local Ethical Committee with a dedicated informed consent. Surplus SV segments, retrieved from patients undergoing CABG were supplied from the Department of Cardiovascular Surgery at Centro Cardiologico Monzino. Samples, after harvesting, were immediately placed at 4°C in DMEM plus 10%FBS, 1% l-Glutamine, 1% penicillin-streptomycin. Before mounting on EVCS vein segments were split in two parts: one portion served as control (Native vein), the second portion was used for the *ex vivo* culture system.

2.2 Ex vivo stimulation protocol. According to our previous report and Chapter II, the EVCS applied a CABG-like pressure stimulation (CABG-PS) with pressure oscillating in the 80-120 mmHg range at a pulse frequency (*f*) of 0.5 Hz. 10-min alternated to 2-min of medium recirculation (flow rate (Q_r): 1 ml/min, with a luminal pressure between 1-2 mmHg). Alternatively, the EVCS applied continuous physiological venous perfusion (VP) with a luminal pressure of 5 mmHg and a flow rate of 3 ml/min. The EVCS was placed within the incubator at 37° C in a 5% CO_2 atmosphere for a culture

period of 7 days. During the culture period, the medium was partially changed at day 3. At day 7 SV segments were un-mounted from the EVCS and were divided in 4 sections for morphometric, immunofluorescence and biochemical studies.

2.3 Histology, immunohistochemistry and immunofluorescence analyses.
Sections were stained with H&E and Masson's trichrome staining according to manufacturer's protocol and digital images were acquired using a light microscope (Axiovert, Carl Zeiss®, Germany) at 10x magnification.
For Ki-67 staining, 3 samples for each group (VP, CABG-PS and related controls) were observed. DAB substrate kit (SK-4100, Vector Laboratories) were used. Slides were incubated with primary Ki-67 antibody 1:100 (Abcam, Cambridge, UK) for 1 hour at room temperature (RT). Slides were counterstained with hematoxylin staining before mounting.
Immunofluorescence (IF) analysis for α-SMA (1:500 monoclonal mouse anti human, Dako), vWF (1:200 polyclonal rabbit anti human, Dako Cytomation), CD31 (1:200 polyclonal goat anti human, Santa Cruz Biotechnology) and CD34 (1:200 monoclonal mouse anti human, Dako) were carried out. These antigens were unmasked using a 10mM Tris-HCL/1mM EDTA/ buffer (pH 9.0) for 10 minutes in microwave. IF for NG2 (1:50 monoclonal mouse anti human, Abcam Cambridge), CD44 (1:500 rat monoclonal anti human, Abcam Cambridge) and SM22α (1:500 polyclonal rabbit anti human, Abcam, Cambridge) were also performed. In this case, antigen unmasking was made by incubating sections for 20 minutes in Target Retrieval Solution (pH 6.0) (Dako) at 90°C. Slides were incubated with secondary antibodies Alexa Fluor 488 anti-mouse, Alexa Fluor 546 anti-goat, Alexa Fluor 546 anti-rat and Alexa Fluor 633 anti-rabbit (1:200; Invitrogen, UK) for 1 hour at RT in 3% BSA, and nuclei were counterstained with DAPI for 15 minutes (Vector Laboratories, CA, USA).
IF to detect histone marks was performed on sections of native and CABG-PS samples (n=3) slices were dewaxed and subjected to microwave for antigen retrieval in a solution of 10 mM TRIS/Citrate/EDTA buffer (pH 7.8). Sections were incubated overnight at 4°C with antibodies (dilution 1:100) (anti-H3K9Ac, Abcam monoclonal; anti-H4K16Ac, Abcam polyclonal; anti-H3K4Me, Abcam polyclonal). Sections were incubated with

FITC or TRITC secondary antibodies (dilution 1:200, Jackson). Nuclei were stained with TOPRO-3 nuclear marker.
Sections incubated with antibodies to detect cellular antigens were observed under a LSM710 confocal microscope equipped with ZEN2010D image acquisition/processing software (Carl Zeiss®); sections stained to detect histone modifications were analysed with a LSM510 Meta confocal microscope (Carl Zeiss®) with 40X magnification.

2.4 Morphometric measurements. Morphometric analyses were performed on Masson's trichrome stained sections as previously reported. The cross sectional area of the sample tissue was estimated assuming a circular shape and using the measured wall thickness and luminal perimeter. The cross sectional area (*A*) was calculated as follows:

$$A = w\,(\pi\, w + p_{inner})$$

where *w* is the wall thickness and p_{inner} is the inner perimeter.
To evaluate the length density of the *vasa vasorum*, H&E stained sections of VP (n=12), CABG-PS (n=12) and relative Native samples were analyzed. Digital images over the entire tissue face were acquired using a light microscope (Carl Zeiss®, Germany) at a magnification of 40x. Using the AxioVision Bio Software (Carl Zeiss®, Germany), the major and minor axes of each *vasum vasorum* were measured. The classification of each vessel was performed based on its minor axis, which, for the definition of length density, represents the vessel diameter. *Vasa vasorum* were subdivided into three subsets: small (4-14 μm), intermediate (14-24 μm), and large (24-44 μm) (2). The *vasa vasorum* length density was calculated for each interval according to:

$$L_d = \frac{\sum_{i=1}^{n} R_i}{A_d}$$

for *n vasa vasorum* counted in a given adventitial area (A_d), the length density (L_d) corresponds to the sum of the ratios (R_i) between the major and the minor axes of each *vasa vasorum*. In addition, *vasa vasorum* displaying no luminal region were not considered for morphometric determination of the length density. The adventitial area (*Ad*) was calculated on digital

micrographs (2.5x) after manual contour identification using GIMP (GNU Image Manipulation Program, Version 2.6.12) and Image-J software (Version 1.47f-sofware for Java, National Institutes of Health, USA).

2.5 Quantification of Ki-67$^+$ cells. A manual counting protocol of Ki-67$^+$ cells was performed by using Image-J software (Version 1.47, National Institutes of Health, USA). The quantitative analysis of positive cells for Ki-67 was accomplished in a blind by only one observer. The number of proliferating cells was normalized to the total cell count in the microscopic fields. In addition, the cell density was evaluated by normalizing the total cell count to the area of the tissue section. The area of the tissue section was calculated on digital micrographs (20x) using Image-J software.

2.6 Protein methods. Zymographic analyses were performed on CABG-PS, VP and Native SVs samples. Frozen tissues were homogenized and samples were centrifuged at 4°C, the supernatant containing proteins was removed and quantified; extracted protein were run in 10% gel electrophoresis containing 1 mg/ml type A Gelatine from porcine skin (SIGMA-Aldrich, Taufkirchen, Germany). To renature proteins, gels were washed two times in 2.5% Triton X-100 and subsequently incubated in developing buffer overnight at 37°C. Gels were stained with Coomassie Blue and destained until clear bands of lytic activity appeared. Image-J software was used for densitometric quantification. Data of MMP-2 were normalized to pro-MMP-2 as internal reference.
Western Blotting analysis was performed on CABG-PS, VP and Native SVs samples. Frozen samples were lysed in Lysis Buffer and extracted proteins were run in a 10% SDS-PAGE, primary antibody solution directed to α-SMA (1:5000 monoclonal mouse anti human, Dako), tissue matrix metallo-proteinases inhibitor-1 (TIMP-1) (1:1000 monoclonal rabbit anti human, Cell Signaling Technology), and GAPDH (1:5000 polyclonal rabbit anti human, Santa Cruz Biotechnology) were used. Image-J software was used for densitometric quantification. Data of α-SMA and TIMP-1 were normalized to GAPDH as internal reference.

2.7 RNA and q-RT-PCR methods. For each miRNA, quantitative real time polymerase chain reaction (q-RT-PCR) was performed using miRNA Reverse Transcription Kit (Applied Biosystems, Foster City, CA) and the

respective primers (miRNA TaqMan Expression assay, Applied Biosystems, Foster City, CA) following the Manufacturer's instructions using a 7900HT Fast Real-Time PCR System (Applied Biosystems, Foster City, CA). We adopted miR-16 as a normalization standard because of its persistent and stable expression throughout all considered samples regardless of the treatment. 500 ng of total RNA was reverse transcribed with Omniscript Reverse Transcrition (Qiagen) according to the manufacturers' instructions. q-RT-PCR was carried out using SYBR green PCR kit (Applied Biosystem) and Applied Biosystems 7900HT Fast Real-Time PCR System. Primers for GAPDH, β_2-Microglobulin, TGF-β_1, BMP-2, Slug and Snail-1 were purchased from Integrated DNA Technologies, while primers for MCP-1 were custom-made and tested in house. Sequences and purchase numbers are shown in Table S1.

Table S1. List of genes tested in Native, VP and CABG-PS stimulated veins.

Gene	IDT Reference #	RefSeqNumber
GAPDH	65558647	NM_002046
B_2M	65558650	NM_004048
TGF-β_1	65558671	NM_000660
BMP-2	65558677	NM_001200
Slug	65558662	NM_003068
Snai1	65558668	NM_005985
MCP-1	-	Fw 5'-ATAGCAGCCACCTTCATTCC-3'
		Rv 5'-ATCCTGAACCCACTTCTGCT-3'

Statistical criteria and analysis. Graph generation and statistical comparisons were performed using Graph-Pad 5 (Prism) software. All data were analysed with D'Agostino and Pearson omnibus normality test and then compared using parametric/non parametric tests (paired/unpaired t-test; one way ANOVA) where appropriate.

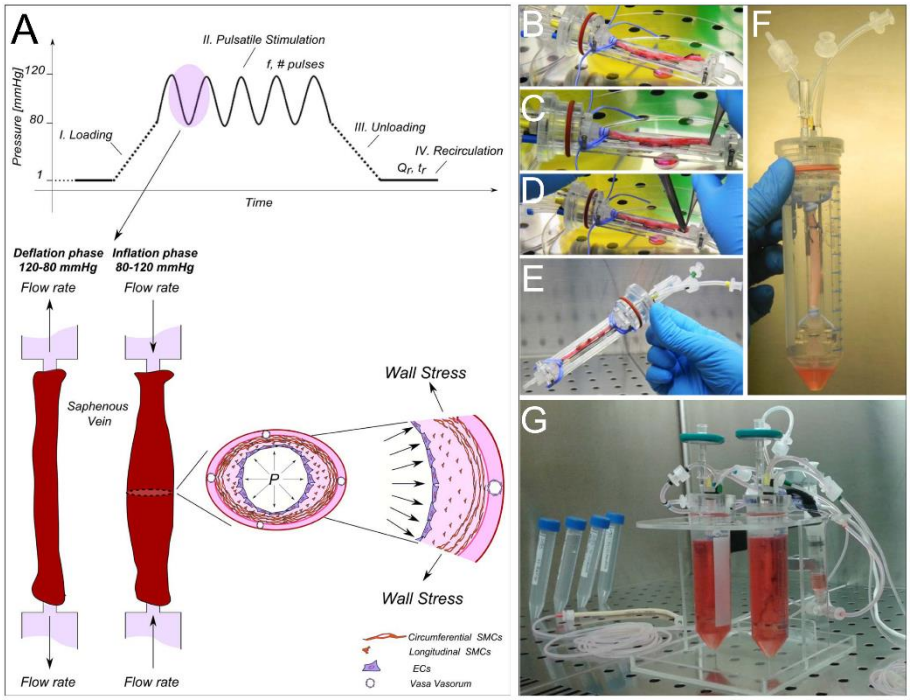

Figure 1. The compact and automated *ex-vivo* vessel culture system able to artificially produce the effects of the pulsatile arterial pressure-related cyclic wall distention. (A) The single pressure stimulation cycle consists of: *i)* a loading phase (the luminal pressure reaches 80 mmHg); *ii)* a pulsatile stimulation phase (pressure oscillates between 80-120 mmHg at a desired pressure rate); *iii)* an unloading phase (pressure is lowered to zero); and *iv)* a recirculation phase with a constant flow rate allowing a metabolic supply to the vessel. The user can set all the specific parameters via the software interface, namely the pressure values, the pulse frequency (*f*) and the number of pulses (*# cycles*) for the pulsatile stimulation period, the duration (t_r) and the medium flow rate (Q_r) for the recirculation period. During the pulsatile stimulation phase (pink spot), the medium is forced into (inflation phase, from 80 to 120 mmHg), or withdrawn (deflation phase, from 120 to 80 mmHg) from the SV sample. During the inflation phase the cells covering the lumen (ECs) and those embedded in the medial layer (SMCs) are subjected to circumferential stress and strain typical of the arterial circulation. (B-E) The EVCS during system assembling under laminar flow hood. The SV segments are cannulated on both ends with barbed luer fittings, and bounded on the connectors using a vessel loop. Then, the SV housing is inserted within the 50-ml tube acting as reservoir (F). Once assembled, the culture chamber is connected to a stimulation circuit (G).

3. Results

The EVCS designed and validated by us (33) performs Coronary Artery Bypass Graft-Pressure Stimulation (CABG-PS) in 4 independent phases (Figure 1A), or Venous Perfusion (VP) conditioning. Briefly, the CABG-PS consists in: *i)* a loading step; *ii)* a pulsatile stimulation step; *iii)* an unloading step; and finally, *iv)* a recirculation step (for more details see Chapter II). During the pulsatile stimulation, a circumferential wall stress is applied to the SV wall. Thus, the cells covering the lumen and those embedded in the medial layer are subjected to circumferential stress and strain typical of the arterial circulation, but in the absence of the elevated shear stress characterizing the coronary flow. VP conditioning consist, instead, in perfusion with culture medium with a constant low pressure (5 mmHg).

3.1 Strain-dependent modifications of the human SV induced by CABG-like pressure patterns. To assess the structural changes occurring in EVCS-cultured human SVs (Figure 1 B-F) in the two conditioning regimens histological analysis was performed. Two major modifications were observed: *i)* a decrease in the vein wall thickness and, *ii)* an increase in the luminal perimeter in CABG-PS *vs.* VP/Native vessels (Figure 2 A-D). While these structural changes were associated to a decrease in the overall cell density, based on nuclei counting (Figure S1A), they did not reflect a generalized tissue wasting, as demonstrated by the lack of a significant decrease in the tissue cross sectional area (35) (Figure S1B).

In previous reports, ex vivo arterial-like conditioning caused an increase in the proliferation of cells in the media and intima layers (32). To confirm this observation in our system, immunolocalization of Ki-67 proliferation marker in native, CABG-PS and VP-conditioned SVs was performed. Results (Figure S2), showed a remarkable elevation of cycling cells only in CABG-PS samples; by contrast, the Ki-67^{+} cells percentage in the VP-treated vessels did not differ from that observed in freshly explanted vessels. Finally, to assess whether CABG-PS causes an increase in Matrix Metalloproteinases MMP-2/-9 activation, and modulates their specific inhibitors (34, 36), zymography and western analyses were made using protein extracts of native and *ex vivo* cultured veins (Fiure S3). A striking increase in MMP-2/-9 activity was observed in both treatments, while the

expression of TIMP-1, the Tissue Inhibitor of Metalloprotease, was upregulated only in VP conditioning of SVs. Taken together, these data suggest the reliability of EVCS to reproduce the biomechanical conditions characterizing vein arterialization.

3.2 The SV adventitia is a direct target of the wall strain in VGD programming. The role of the adventitia as a crucial regulator of vessel homeostasis (37) has recently emerged. Its contribution to intimal thickening has been mainly investigated in animal models (9, 22, 25, 38). Quantification of *vasa vasorum* growth was performed by establishing three size categories (small 4-14µm, intermediate 14-24µm and large 24-44µm) followed by length density determination (39). This helped us to discriminate between the formation of novel vessels (small) *vs.* growth of preexisting adventitial vascular structures (intermediate and large). As shown in Figure 2 E-F, none of the three groups were affected in VP treated vessels. By contrast, in CABG-PS SVs, a significant increase in the length density of the 24-44µm vessels was observed, suggesting that the hypertrophic response was the result of pre-existing vessel growth. Interestingly, an increase in Ki-67^{+} cells presence was also noticed in the *vasa vasorum* of CABG-PS SVs (Figure 2G). To monitor whether the increase in the *vasa vasorum* density was associated with changes in markers expression, an immunofluorescence analysis was performed using antibodies directed against endothelial cells (ECs) (CD31, vWF), SMCs (αSMA) markers. In particular, the CABG-PS veins showed hypertrophic *vasa vasorum* surrounded by multiple cellular layers (Figure 3C, see also 2E). This was opposite to the structure of the *vasa vasorum* in the native vessel, where only one/two cell layers were observed (Figure 3A, see also 2E).

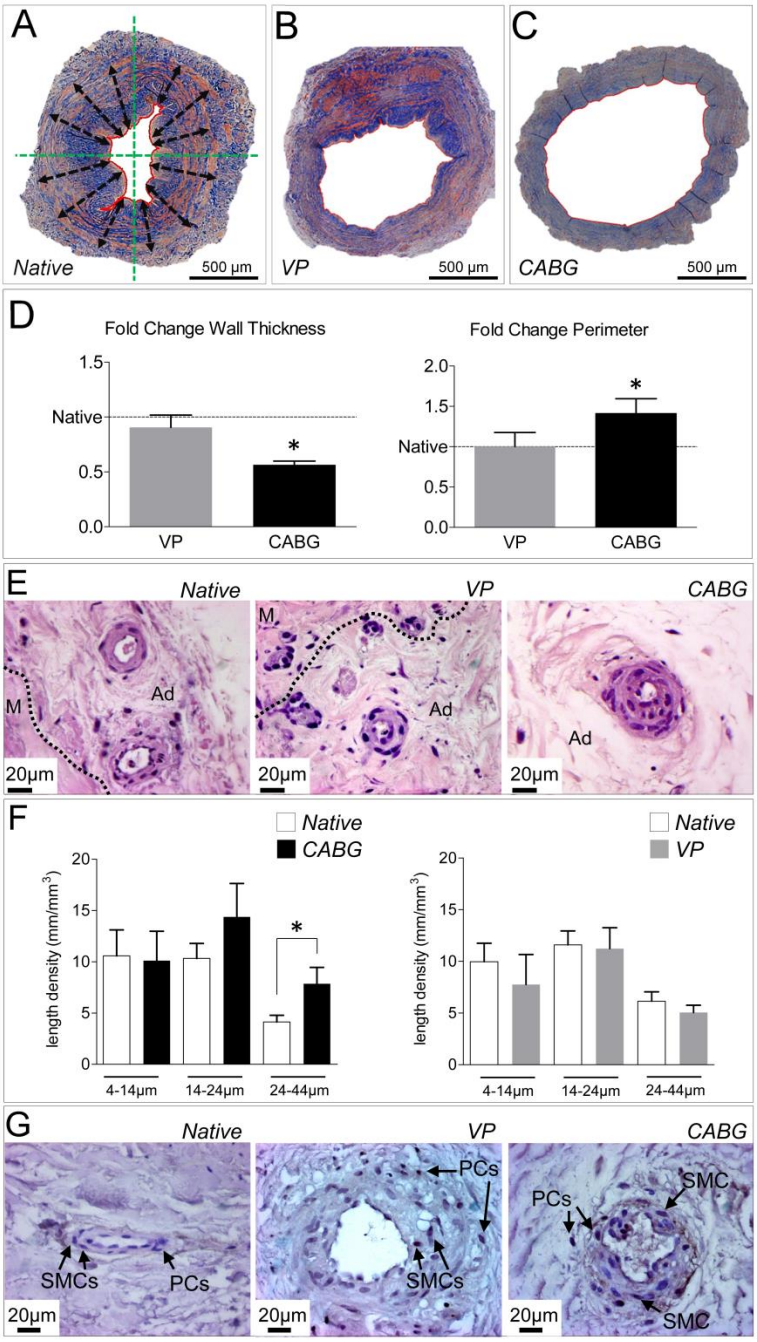
A
Native
500 µm
B
VP
500 µm
C
CABG
500 µm
D
Fold Change Wall Thickness
1.5
Native
0.5
0.0
*
VP
CABG
Fold Change Perimeter
2.0
1.5
Native
0.5
0.0
*
VP
CABG
E
Native
VP
CABG
M
Ad
20µm
M
Ad
20µm
Ad
20µm
F
Native
CABG
length density (mm/mm3)
20
15
10
5
0
*
4-14µm
14-24µm
24-44µm
Native
VP
length density (mm/mm3)
20
15
10
5
0
4-14µm
14-24µm
24-44µm
G
Native
VP
CABG
SMCs
PCs
20µm
PCs
SMCs
20µm
PCs
SMC
SMC
20µm

Figure 2. (A-C) Low magnification of Masson's thrichrome staining of SV transversal sections. The arrows in A indicate the direction of the radial measures used to determine wall thickness. (D) Quantification of wall thickness and luminal perimeter changes in VP and CABG-PS samples *vs.* controls (Native). Data are expressed as fold change *vs.* control (set to 1 in the graphs); * indicates $P < 0.05$ by paired t-test *vs.* controls (n=6). (E) Representative micrographs of the adventitial layer in Native, VP and CABG-PS SVs stained with H&E. The structure of the *vasa vasorum* is shown. Note the relatively higher thickness of these structure in CABG-PS *vs.* VP and native veins. The boundary between the media (M) and the adventitia layers (Ad) is shown. (F) Quantification of *vasa vasorum* length density in the adventitia (39). No difference was found in the density of these structures in VP, while the 24-44μm category was significantly increased in CABG-PS samples. * indicates $P < 0.05$ by paired t-test (n=12 CABG-PS samples; n=12 VP samples). (G) Representative images of *vasa vasorum* immunostaining with the Ki-67 antibody. Note the higher presence of Ki-67^{+} positive cells at the periphery of these vessels (arrows) in CABG-PS *vs.* native and VP veins. Cells with a smooth muscle cell (SMC) and pericyte (PC) localization are indicated by arrows.

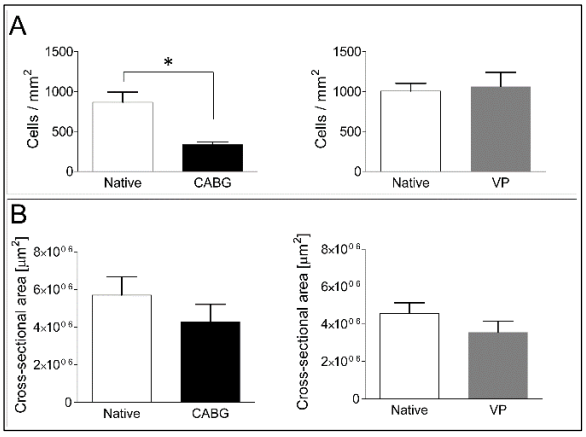

Figure S1. (A) Evaluation of cell number/mm^2 in Native *vs.* CABG-PS and Native *vs.* VP cultured SVs. * indicates $P < 0.05$ by unpaired t-test (n=3). (B) Cross sectional area evaluation (4) in Native *vs.* CABG-PS and Native *vs.* VP cultured SVs. Data comparison by unpaired t-test (n=6) did not show statistically significant differences.

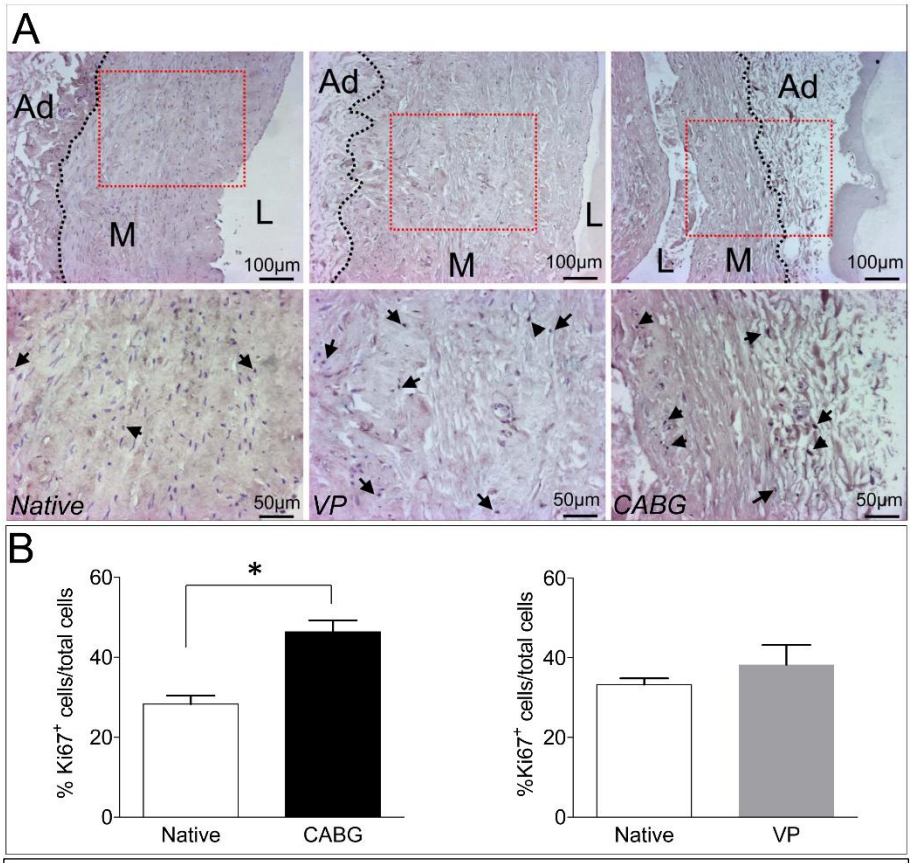

Figure S2. (A) Low and high magnification of immunohistochemical staining for Ki-67 proliferation marker in Native, VP and CABG-PS veins. Arrows indicate cell nuclei expressing Ki-67. L: lumen, M: media, Ad: adventitia. (B) Quantification of Ki-67$^+$ cells, expressed as a percentage of the total in Native *vs.* CABG-PS and Native *vs.* VP cultured SVs. * indicates $P < 0.05$ by unpaired t-test (n=3).

In VP treated vessels, a situation similar to native SVs was found, with vessels having a normal structure (Figure 3B, see also 2E). However, the most striking changes were observed in the CABG-PS *vasa vasorum*, with an evident disarrangement of the microvascular structure, decrease in the level of SMCs and ECs markers, and larger nuclei. In addition, in CABG-PS SVs, αSMA$^+$ cells appeared to loose contact with the *vasa vasorum* structure and to invade the surrounding adventitia (Figure 3C). IF analysis allowed also the recognition of the so called saphenous vein progenitors (SVPs) (21) characterized by CD34 but not CD31 and vWF expression (21). Participation

of adventitial progenitor cells to VGD and, more in general, to stenosis after vascular damage has been shown so far only in animal models (9, 28, 40-42).

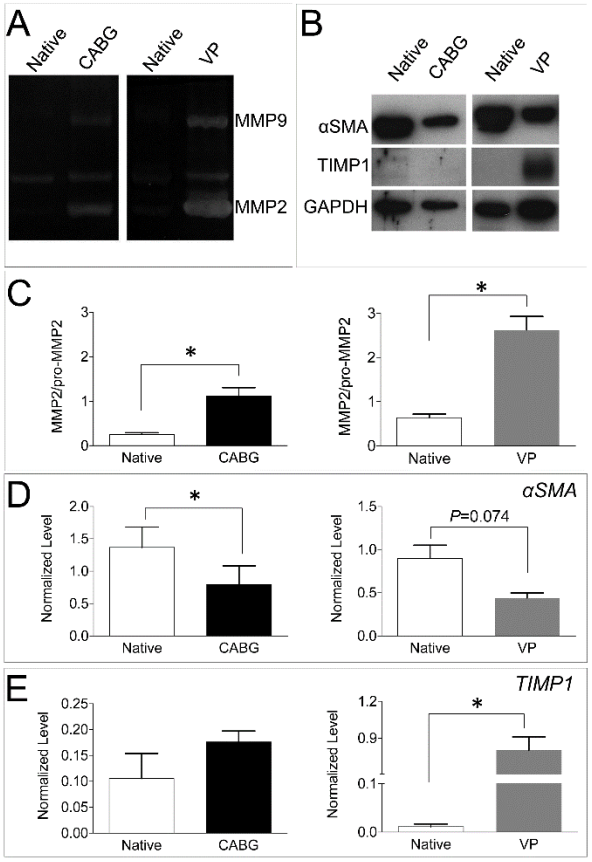

Figure S3. (A) Zymography of MMP2/9 and (B) α-SMA/TIMP-1 Western Blot analysis in protein extracts from Native, VP and CABG-PS cultured SVs. (C-E) Quantification and statistical comparison of the MMP2 activity (n=5) (C), α-SMA (n≥3), (D) and TIMP-1 (n≥3) expression in Native *vs.* CABG-PS and Native *vs.* VP samples. * indicates $P < 0.05$ by paired t-test. The *P* value above graphs is indicated in case of a borderline statistical significance by paired t-test (D).

Given increasing interest for the homeostatic function of the vascular adventitia, even in the human system (26, 27, 43), it was particularly interesting to assess the fate of the perivascular resident progenitors in the SV segments undergoing mechanical straining. The observation of the immunofluorescence staining in SV tissue sections revealed no changes in the content of cells clearly recognizable as SVPs. In fact, the number of $CD34^{+}/CD31^{-}/vWF^{-}$ cells in CABG appeared to be barely modified (Figure

3). Since vascular pericytes and SVPs are also characterized by expression of NG2 (21, 44), we then performed immunofluorescence to localize this marker in the tissue sections. This was done in conjunction with antibodies recognizing CD44, a marker abundantly expressed in vascular mesenchymal cells (25) and SM22α, a marker of muscle cells. As shown in Figure 4A, and consistently with other reports (21, 44), the expression of these markers was low in the native vessels. By contrast, an evident upregulation of NG2 and SM22α was observed in the outer cells ring in *vasa vasorum* of VP- and CABG-PS trained veins. Finally, groups of $NG2^{+}/SM22\alpha^{+}/CD44^{+}$ cells located in proximity of the boundary between the adventitia and the media were found in CABG-PS veins only.

3.3 Modified epigenetic marking in *vasa vasorum* of CABG-PS trained SVs. The involvement of promoter-specific methylation of histone H3 in perivascular cells contributing to vessel atherosclerosis has been recently demonstrated (46). To assess whether the CABG-PS was associated to changes in epigenetic marks, a method to detect different histones H3/4 methylation/acetylation (47) was used. In a survey of 5 histone marks involved in generalized gene transcriptional activation or repression (48), mono-methylation of the lysine 4 on histone H3 (H3K4me) and acetylation of lysines 9 and 16 on histone H4 (H4K9Ac, H4K16Ac) were significantly increased in CABG-PS *vs.* Native vessels (Figure 4B-C). Interestingly, these modifications were mainly observed in adventitial cells and in cells of the *vasa vasorum*.

3.4 Wall strain-dependent gene expression in human SV. The upregulation of various micro-RNAs has been highlighted in recent reports as an important component in vascular stenosis (49), vein graft failure (18, 19) and, more in general, cardiovascular diseases (50, 51). In order to assess whether culture of the SV in the EVCS recapitulates the miRNA-dependent pathology programming observed in previous studies, and to screen for biomechanical-specific gene expression activation, q-RT-PCR was performed on total RNA extracted from Native, VP and CABG-PS veins. In our analysis, three differentially regulated miRNAs categories were found: *i)* miRNAs upregulated in VP and CABG-PS treated veins (miR-21/146a/221; Figure 5A); *ii)* miRNAs upregulated in CABG-PS but not in VP-treated SVs

(miR-138/200b/200c; Figure 5B) and *iii)* one miRNA (miR-133a), that was downregulated more pronouncedly in VP than in CABG-PS samples (Figure 5C). The other tested miRNAs (miR-24/34a/126/145) were not modified in any of the tested conditions.

Various paracrine and chemotactic signaling pathways orchestrate vascular inflammation and IH in VGD. This is the example of the Sonic Hedgehog (Shh) dependent pathway, which directs SMCs proliferation in arterialized veins in mice (52), or that of the chemokine MCP-1, that promotes intimal migration of SMCs and cells with pericyte characteristics (24). In addition, the observed increase in miR-21/200b/200c expression suggested an implication of the TGF-β-dependent pathway (53, 54). In order to clarify whether mechanical stimulation is a sufficient trigger to activate other paracrine signaling involved in vessel pathologic progression and activation of adventitial progenitors, a q-RT-PCR was performed to determine the expression level of *Shh*, *MCP-1*, *TGF-β_1*, *BMP-2* - a factor involved in SMCs calcification (55), and *ZEB-1*, *SLUG* and *SNAIL* - transcription factors involved in Shh signaling (56). As shown in Figure 5D, *TGF-β_1* and *BMP-2* were the only significantly modulated targets in CABG-PS *vs.* VP-treated and Native samples. Surprisingly, the other tested genes were unchanged during *ex vivo* culture or not expressed.

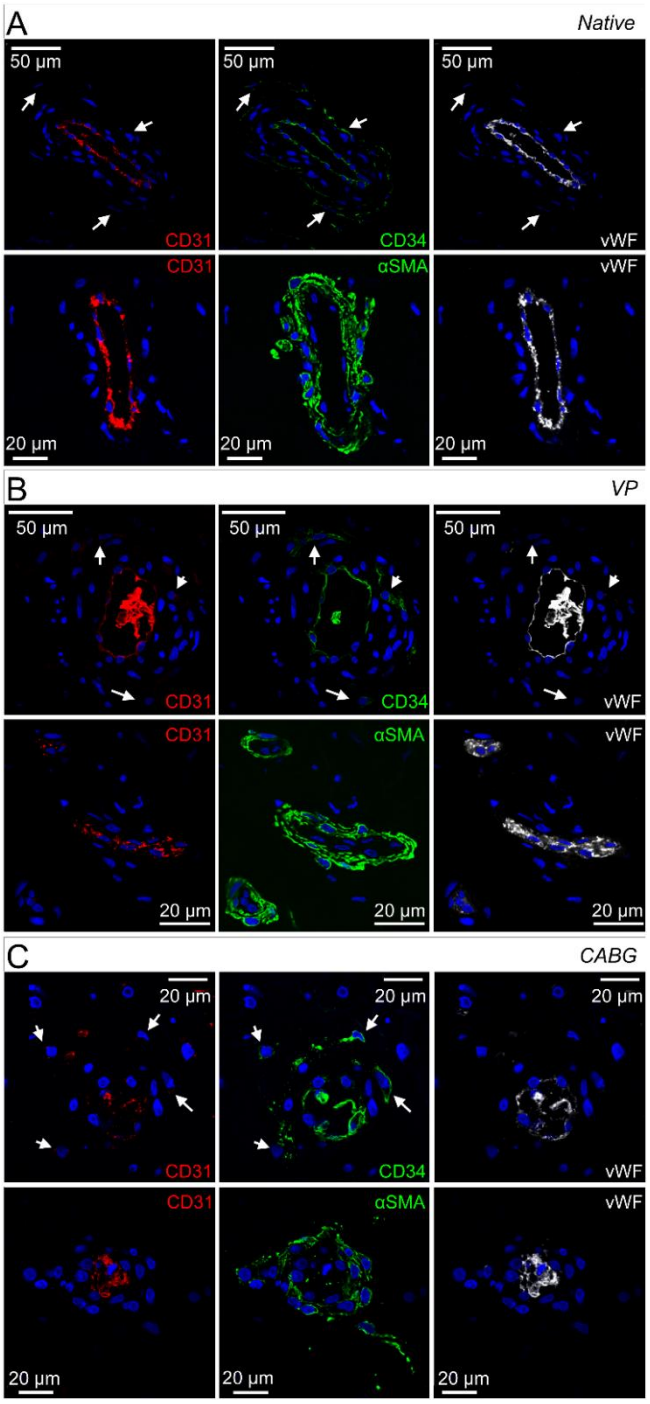

Figure 3. Confocal microscopy analysis of triple staining with CD31/CD34/vWF or CD31/αSMA/vWF antibodies to detect cells with a pericyte and SMC phenotype in the *vasa vasorum* in Native (A), VP- (B) or CABG-PS (C) SVs. While the presence of cells with SVP (21) characteristics ($CD34^+/CD31^-/vWF^-$) appeared not to be different among treatments (arrows), a decrease in EC markers in the *vasa vasorum* luminal endothelial cells, as well as α-SMA in the surrounding SMCs was observed in vasa vasorum of CABG-PS *vs.* VP and native samples. In addition, the *vasa vasorum* in CABG-PS treated *vs.* VP and native samples appeared remarkably de-structured with cells migrating out of them (see also video S2 for additional information)

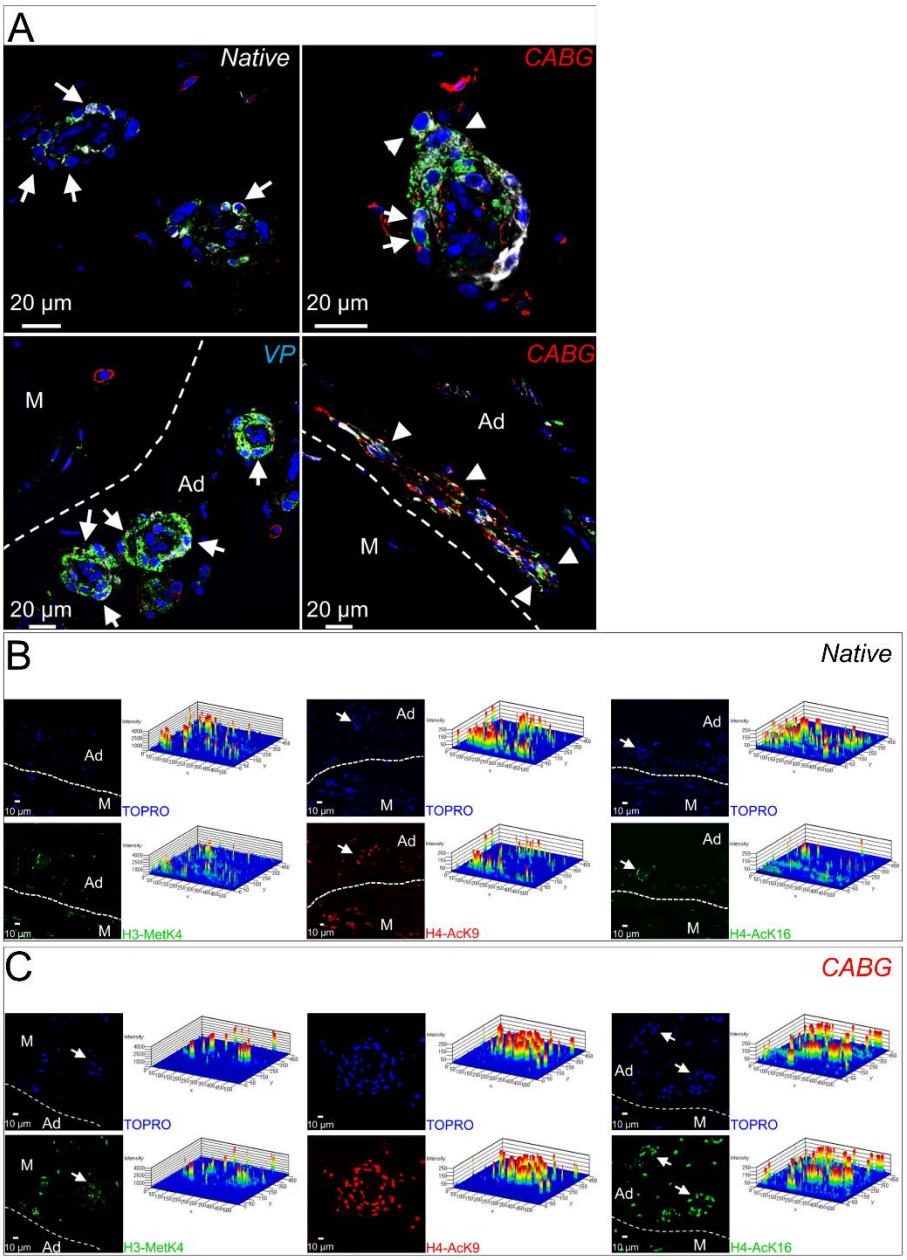
A
Native
CABG
20 µm
20 µm
VP
CABG
M
Ad
Ad
M
20 µm
20 µm
B
Native
Ad
M
TOPRO
H3-MetK4
H4-AcK9
H4-AcK16
C
CABG
TOPRO
H3-MetK4
H4-AcK9
H4-AcK16

Figure 4. (A) Confocal microscopy analysis of triple stained Native, VP and CABG-PS samples with antibodies against NG2 pericyte marker (green fluorescence) SM22α (white fluorescence) and CD44 (red fluorescence). The expression of NG2 and SM22α was confined to a pericyte-like ring of cells located at the periphery of the *vasa vasorum*, while a higher expression of both markers was found either in VP or CABG-like samples. Note the presence of cells expressing NG2 and SM22α markers 'budding' from the *vasa vasorum* wall (upper right panel, arrowheads) in CABG-PS treated vein. Only in CABG-PS samples, abundant cells expressing NG2/SM22α/CD44 were found at the boundary between the adventitia (Ad) and the media (M), indicated by a bracketed line. (B-C) The methylation/acetylation level of the histones H3/H4 was investigated by immunofluorescence/confocal microscopy in Native (B) and CABG-PS (C) samples. The results of this analysis revealed increased histone H3 methylation on Lysine 4 (H3-MetK4) and Histone H4 acetylation at Lysines 9 and 16 (H4-AcK9; H4-AcK16). Panels show the microscopic fields stained with the indicated antibodies and the relative quantification of the fluorescence in the nuclei (TOPRO) and histone modification relative channels, represented with a 2.5 dimension projection of the fluorescence intensity in the field. Arrows indicate the cells present in the *vasa vasorum*, while the bracketed lines show the boundary between the media (M) and the adventitia (Ad) layers.

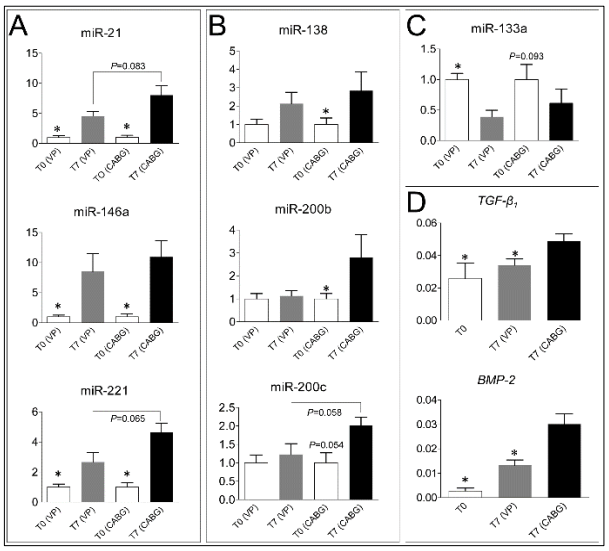

Figure 5. Assessment of biomechanical-dependent and -independent transcriptional regulation in the human SV. (A) q-RT-PCR experiment showing expression of miR-21/146a/221 in native (T0) VP and CABG-PS samples. Graphs show the fold changes observed in the expression of each micro-RNA (calculated by $2^{-\Delta\Delta CT}$) in order to compare the samples series (VP or CABG-PS) with their relative control series [T0 (VP) or T0 (CABG)], by using paired non-parametric t-test (Wilcoxon matched-pairs signed rank test), and perform inter group (VP *vs.* CABG-PS) comparison using unpaired non-parametric t-test (Mann-Whitney). * above control bars indicate a $P < 0.05$ value in the comparison between treatments and controls, while numbers associated to connecting lines between bars indicate the *P* values achieved in the unpaired statistical tests adopted to compare the miRNAs expression in CABG-PS *vs.* VP treatments. (B) Expression of biomechanically-regulated microRNAs (miR-138/200b/200c) in SVs exposed to CABG-PS, but not VP condition. Data are expressed and grouped as in panel A. * above control bars indicate a $P < 0.05$ value ($P = 0.054$ for miR-200c) in the comparison between treatments and controls by Wilcoxon matched-pairs signed rank test, while the number associated to connecting lines between bars in the miR-200c graph indicates the *P* value rendered by the unpaired statistical test adopted to compare the miRNAs expression in CABG-PS *vs.* VP treatments. (C) miR-133a expression was reduced by the VP, but not CABG-PS treatment. Data grouping, statistical comparison and level of significance as above. (D) TGF-β_1 and BMP-2 expression are elevated in CABG-PS but not VP treated samples. Gene expression data are represented as relative expression ($2^{-\Delta CT}$) and were compared using one way ANOVA with Newman-Keuls post-hoc analysis. * above bars indicate a $P < 0.05$ value rendered by the statistical test.

4. Discussion

We already validated and published the design of a novel EVCS able to stimulate vein segments with arterial-like pattern pressure. In this second contribution we adopted the EVCS to investigate the vessel arterialization process under a structural, cellular and molecular point of view. The results obtained by MMP-2/-9 activation are in line with studies performed in animal models or previous ex vivo human vessel culture systems (34, 65)

The contribution of various growth factors/chemokines (57-60), extracellular matrix remodelling enzymes (57, 61), intracellular gene activation pathways (62) and gene expression signatures (18) in VGD have been highlighted in animal models of vein arterialization (8). This has led to preclinical/clinical experimentation (16), mostly based on gene transfer approach, whose translational outcomes are, unfortunately, still unsatisfactory (63). The limited efficacy of the intervention strategies devised until now may derive from the underestimation of important pathology causes, such as biomechanical factors. In fact, not only the modified fluid shear stress at the level of the endothelial cells, but also the altered wall strain consequent to the switch from a low/constant pressure to a high/pulsatile pressure regime in the graft, may have important effects in the establishment and progression of the pathology (64). In this regard, the evolution of systems tailored to perform an accurate modelling of the biomechanical forces in vein graft failure using human samples (32, 34), represents a milestone in a comprehensive understanding of the disease at a molecular level.

4.1 Structural remodelling and biochemical changes in *ex vivo* arterialized veins reveals an effect of wall strain on early pathologic SV programming. Despite the clinical manifestation of the vein graft patency reduction occurs at relatively late stages after implantation, the disease process is believed to start within hours after implantation, with a crucial contribution of mechanical forces (4). For this reason, culturing SVs for a limited amount of time under the appropriate biomechanical conditions is considered sufficient to recapitulate the early events occurring in VGD. The adoption of a perfusion protocol consistent with the normal vein flow

characteristics (the VP condition) enabled us to operate important discriminations between the changes occurring in the vein due to surgical manipulation and tissue culture *vs.* those attributable to pure biomechanical effects. For example, the analysis of MMP2/9 activation did not show remarkable differences between the two culturing conditions (Fig. The EVCS adopted in the present study was used to expose segments of the human SV to a pulsatile pressure with the biomechanical characteristics of the coronary artery flow (33) using a relatively simple stimulation protocol for a period of 7 days. In keeping with previous reports showing similar approaches (32), the system induced structural changes in the vessel consistent with those reported in vascular conduits used in patients (20, 31). These included an around 45% reduction of the wall thickness and a consequent 45% increase in the luminal perimeter in CABG-like stimulated veins (Fig. 2 A-D). This event was accompanied by a significant cell loss (measured by the decrease of the total nuclei density, Fig. S1A), probably due to strain-dependent programmed cell death (36) in circumferential SMCs sheets (Fig. 2C). With the present contribution we cannot affirm if this cell loss is caused by a process of cellular death due to necrosis, apoptosis or autophagy; however, it was not associated to a decrease in the tissue cross sectional area (Fig. S1B). This latter result, together with the increased presence of Ki-67^{+} cells in the wall of CABG-PS treated veins (Fig. S2), and with the demonstrated ability of the system to maintain the overall vessel viability (33), indicates that the observed remodeling was the result of an active adaptation process, and not of an unspecific tissue degeneration consequent to non-optimized culture conditions. The consistent downregulation in TIMP-1 protein level only in CABG-PS veins (Fig. S3B, E) suggests, for the first time, a direct effect of the arterial-like wall strain on suppression of important factors protecting from vessel remodeling. Whether TIMP-1 suppression occurs by transcriptional repression or by an epigenetic/microRNAs circuitry, is the subject of our ongoing investigations.

4.2 Strain-dependent/-independent miRNA and transcriptional circuitries in vein arterialization process. A new therapeutic perspective in vein graft stenosis has been offered by recent implication of miRNAs in VGD setting and progression (18, 19). In particular, the involvement of miR-21 was very interesting, given its implication in cardiac fibrosis,

endothelial/epithelial to mesenchyme transition and flow-dependent or damage-dependent vascular remodeling (50, 54, 66-68). For this reason, we assessed whether the expression of miR-21, and of other miRNAs putatively engaged in mechanical stress-dependent (67) or -independent (50, 69) vascular pathology process, was affected by exposure of the SV to wall strain. The results delineated a very interesting scenario, in which the expression of miR-21/221 was enhanced (although with a borderline significance) in CABG-PS *vs.* VP samples (Figure 5A), and other miRNAs (138/200b/200c) were specifically upregulated in the presence of wall strain. We already do not know the role that these latters micro RNAs exert during the early events of IH, they may be beneficial for IH inducing/sustaining its development or they may be signals act to avoid/delay the pathology. We found one micro RNA (mir-133) downregulated specifically after 7 days of venous perfusion, this could be an important element to consider because it is modulated in venous physiologic stimulation. It is possible that mir-133 must be dowregulated to preserve the venous identity of the graft avoiding the arterialization process.
The set of micro RNAs (mir-21, -146a, -221) upregulated both in CABG-PS and VP conditioning, point out the presence of signals triggered by the tissue isolation, harvesting and 7days of *ex vivo* culture.

Given the tight interrelationship between these targets and the TGF-β-dependent signaling in cardiovascular disease (54, 70), we determined whether transcriptional regulation of this factor was also under the control of the arterial-like wall strain. We tested also the expression of other genes (Table S1) important in the vessel remodeling events, it was interesting to find that TGF-β_1 and BMP-2 were significantly elevated in CABG-stimulated, but not in VP-treated veins. TGF-β is a well-known signal that promotes vein intimal hyperplasia, infact it involves proliferation, survival, differentiation and migration of SMCs. Taken together, these results suggest, an involvement of miR-21/221-dependent pathologic programming (19) by a biomechanically-regulated miRNAs circuitry (miR138/200b/200c). This genes activation in CABG-PS veins potentially involves epithelium/endothelium mesenchymal transitions (72), vascular stress (73) or inflammatory (74) pathways. At the present stage of the research, the functional relevance of these circuitries is still speculative, given the

surprising absence of a coherent *SLUG*, *SNAIL* and *ZEB-1* regulation in strained SVs.

4.3 From biomechanics to activation of vessel-resident cells: a novel mechanism in neointima hyperplasia in vein grafts? Increase in the *vasa vasorum* density in the adventitia of veins grafts has been described as a *neo*-vascularization process occurring in response to the sudden ischemia caused by the loss of blood supply at the time of vein excision (75); more recently, it has been proposed as a crucial IH component after vascular injury (76, 77). The stimulation conditions (VP and CABG-PS) adopted in the present study were set to avoid oxygen availability differences between the adventitial and the luminal surface of the veins. This prevented adventitial hypoxia to cause interferences in the biological responses of the SV tissue. For this reason, we interpret the increase in the *vasa vasorum* length density observed in the CABG-PS SV segments (Fig. 2 F-G) as another direct effect of the biomechanical strain. This is also consistent with: i) the remarkable morphological chenges in these vessels revealed by immunofluorescence experiments (Fig. 3), ii) the appearance, only in CABG-PS vein, of cells expressing pericyte marker NG2 (44, 78) in conjunction with SM22α and CD44 at the boundary between the adventitial and medial layer (Fig. 4A), and, iii) the presence of transcriptional permissive epigenetic marks (48), in CABG-PS veins (Fig. 4B-C). This latter result is consistent with an outgrowth of a pericyte-derived cellular population arising from disarrangement of adventitial *vasa vasorum* consequent to mechanical strain revealed by immunofluorescence experiments (Fig. 3).

Finally, given the recent appraisal of the vascular adventitia as a niche for multipotent progenitors engaged in vascular pathology process (26), and the involvement of adventitial progenitors in intima hyperplasia in animal models of vein arterialization (9, 22), our results indicate a biomechanically-driven pathologic commitment of adventitial progenitors in the human pathology. We cannot definitively conclude, at the moment, whether progenitor cells resident in the SV adventitia are a direct target of the arterial-like mechanical strain, or whether they are activated by a paracrine signaling established in the vein wall as a result of altered mechanosensing in SMCs. While we are currently exploring the first possibility by testing the

effect of pathologic mechanical strain on isolated SVPs in culture (21), the data showing the biomechanic-driven activation of TGF-β/BMP-2/miRNA circuitries are consistent with the second hypothesis.

In summary, the present contribution highlights, for the first time, the involvement of the arterial-like wall strain in the VGD molecular setting in the human tissue. In addition to consolidate observations up to date possible only in animal models (22), our engineering approach offers a validated and a novel investigational method based on biomechanics-related target assessment to proceed with more refined vessel preconditioning strategies and translational interventions.

5. References

1. Konstantinov IE (1997) The First Coronary Artery Bypass Operation and Forgotten Pioneers. *The Annals of Thoracic Surgery* 64(5):1522-1523.
2. Wallitt EJ, Jevon M, & Hornick PI (2007) Therapeutics of vein graft intimal hyperplasia: 100 years on. *Ann Thorac Surg* 84(1):317-323.
3. Kim FY, Marhefka G, Ruggiero NJ, Adams S, & Whellan DJ (2013) Saphenous vein graft disease: review of pathophysiology, prevention, and treatment. *Cardiol Rev* 21(2):101-109.
4. Shukla N & Jeremy JY (2012) Pathophysiology of saphenous vein graft failure: a brief overview of interventions. *Current Opinion in Pharmacology* 12(2):114-120.
5. Dashwood MR & Tsui JC (2013) 'No-touch' saphenous vein harvesting improves graft performance in patients undergoing coronary artery bypass surgery: A journey from bedside to bench. *Vascular Pharmacology* 58(3):240-250.
6. Johansson BL, *et al.* (2010) Slower progression of atherosclerosis in vein grafts harvested with 'no touch' technique compared with conventional harvesting technique in coronary artery bypass grafting: an angiographic and intravascular ultrasound study. *Eur J Cardiothorac Surg* 38(4):414-419.
7. Locker C, *et al.* (2012) Multiple Arterial Grafts Improve Late Survival of Patients Undergoing Coronary Artery Bypass Graft Surgery: Analysis of 8622 Patients With Multivessel Disease. *Circulation* 126(9):1023-1030.
8. Thomas AC (2012) Animal models for studying vein graft failure and therapeutic interventions. *Current Opinion in Pharmacology* 12(2):121-126.
9. Hu Y, *et al.* (2004) Abundant progenitor cells in the adventitia contribute to atherosclerosis of vein grafts in ApoE-deficient mice. *J Clin Invest* 113(9):1258-1265.
10. Torsney E, Hu Y, & Xu Q (2005) Adventitial progenitor cells contribute to arteriosclerosis. *Trends Cardiovasc Med* 15(2):64-68.
11. Fogelstrand P, Osterberg K, & Mattsson E (2005) Reduced neointima in vein grafts following a blockage of cell recruitment from the vein and the surrounding tissue. *Cardiovasc Res* 67(2):326-332.
12. Zhang L, Peppel K, Brian L, Chien L, & Freedman NJ (2004) Vein graft neointimal hyperplasia is exacerbated by tumor necrosis factor receptor-1 signaling in graft-intrinsic cells. *Arterioscler Thromb Vasc Biol* 24(12):2277-2283.
13. Zhang L, Freedman NJ, Brian L, & Peppel K (2004) Graft-extrinsic cells predominate in vein graft arterialization. *Arterioscler Thromb Vasc Biol* 24(3):470-476.
14. Kudo FA, *et al.* (2007) Venous identity is lost but arterial identity is not gained during vein graft adaptation. *Arterioscler Thromb Vasc Biol* 27(7):1562-1571.
15. Southerland KW, Frazier SB, Bowles DE, Milano CA, & Kontos CD (2013) Gene therapy for the prevention of vein graft disease. *Translational Research* 161(4):321-338.
16. Robertson KE, McDonald RA, Oldroyd KG, Nicklin SA, & Baker AH (2012) Prevention of coronary in-stent restenosis and vein graft failure: Does vascular gene therapy have a role? *Pharmacology & Therapeutics* 136(1):23-34.
17. Wiedemann D, *et al.* (2012) Perivascular administration of drugs and genes as a means of reducing vein graft failure. *Current Opinion in Pharmacology* 12(2):203-216.
18. McDonald RA, Hata A, MacLean MR, Morrell NW, & Baker AH (2012) MicroRNA and vascular remodelling in acute vascular injury and pulmonary vascular remodelling. *Cardiovascular Research* 93(4):594-604.
19. McDonald RA, *et al.* (2013) miRNA-21 is dysregulated in response to vein grafting in multiple models and genetic ablation in mice attenuates neointima formation. *European Heart Journal*.
20. Owens CD (2010) Adaptive changes in autogenous vein grafts for arterial reconstruction: clinical implications. *J Vasc Surg* 51(3):736-746.

21. Campagnolo P, *et al.* (2010) Human adult vena saphena contains perivascular progenitor cells endowed with clonogenic and proangiogenic potential. *Circulation* 121(15):1735-1745.
22. Chen Y, *et al.* (2013) Adventitial Stem Cells in Vein Grafts Display Multilineage Potential That Contributes to Neointimal Formation. *Arteriosclerosis, Thrombosis, and Vascular Biology*.
23. Corselli M, *et al.* (2012) The tunica adventitia of human arteries and veins as a source of mesenchymal stem cells. *Stem cells and development* 21(8):1299-1308.
24. Grudzinska MK, *et al.* (2013) Monocyte Chemoattractant Protein 1–Mediated Migration of Mesenchymal Stem Cells Is a Source of Intimal Hyperplasia. *Arteriosclerosis, Thrombosis, and Vascular Biology* 33(6):1271-1279.
25. Klein D, *et al.* (2011) Vascular wall-resident CD44+ multipotent stem cells give rise to pericytes and smooth muscle cells and contribute to new vessel maturation. *PLoS ONE* 6(5):e20540.
26. Majesky MW, Dong XR, Hoglund V, Daum G, & Mahoney WM, Jr. (2012) The adventitia: a progenitor cell niche for the vessel wall. *Cells Tissues Organs* 195(1-2):73-81.
27. Majesky MW, Dong XR, Hoglund V, Mahoney WM, & Daum G (2011) The Adventitia. *Arterioscler Thromb Vasc Biol* 31(7):1530-1539.
28. Tang Z, *et al.* (2012) Differentiation of multipotent vascular stem cells contributes to vascular diseases. *Nat Commun* 3:875.
29. Sankaran S, *et al.* (2012) Patient-Specific Multiscale Modeling of Blood Flow for Coronary Artery Bypass Graft Surgery. *Annals of Biomedical Engineering* 40(10):2228-2242.
30. McGah PM, *et al.* (2012) Hemodynamic conditions in a failing peripheral artery bypass graft. *Journal of Vascular Surgery* 56(2):403-409.
31. Gasper WJ, *et al.* (2013) Thirty-day vein remodeling is predictive of midterm graft patency after lower extremity bypass. *Journal of Vascular Surgery* 57(1):9-18.
32. Piola M, *et al.* (2012) Tools and procedures for ex vivo vein arterialization, preconditioning and tissue engineering: a step forward to translation to combat the consequences of vascular graft remodeling. *Recent Pat Cardiovasc Drug Discov* 7(3):186-195.
33. Piola M, *et al.* (2013) A compact and automated ex vivo vessel culture system for the pulsatile pressure conditioning of human saphenous veins. *Journal of tissue engineering and regenerative medicine*.
34. Berard X, *et al.* (2013) Role of hemodynamic forces in the ex vivo arterialization of human saphenous veins. *Journal of Vascular Surgery* 57(5):1371-1382.
35. Tran-Son-Tay R, *et al.* (2008) An Experiment-Based Model of Vein Graft Remodeling Induced by Shear Stress. *Annals of Biomedical Engineering* 36(7):1083-1091.
36. Wong AP, *et al.* (2008) Expansive remodeling in venous bypass grafts: Novel implications for vein graft disease. *Atherosclerosis* 196(2):580-589.
37. Stenmark KR, *et al.* (2013) The adventitia: essential regulator of vascular wall structure and function. *Annual review of physiology* 75:23-47.
38. Passman JN, *et al.* (2008) A sonic hedgehog signaling domain in the arterial adventitia supports resident Sca1+ smooth muscle progenitor cells. *Proc Natl Acad Sci U S A* 105(27):9349-9354.
39. Pesce M, *et al.* (2003) Myoendothelial differentiation of human umbilical cord blood-derived stem cells in ischemic limb tissues. *Circ Res* 93(5):e51-62.
40. Hu Y, *et al.* (2002) Both donor and recipient origins of smooth muscle cells in vein graft atherosclerotic lesions. *Circ Res* 91(7):e13-20.
41. Hu Y & Xu Q (2011) Adventitial Biology. *Arterioscler Thromb Vasc Biol* 31(7):1523-1529.
42. Daniel J-M, *et al.* (2010) Time-Course Analysis on the Differentiation of Bone Marrow-Derived Progenitor Cells Into Smooth Muscle Cells During Neointima Formation. *Arteriosclerosis, Thrombosis, and Vascular Biology* 30(10):1890-1896.
43. Hoglund VJ, Dong XR, & Majesky MW (2010) Neointima formation: a local affair. *Arterioscler Thromb Vasc Biol* 30(10):1877-1879.

44. Crisan M, *et al.* (2008) A Perivascular Origin for Mesenchymal Stem Cells in Multiple Human Organs. *Cell Stem Cell* 3(3):301-313.
45. Lockman K, Taylor JM, & Mack CP (2007) The Histone Demethylase, Jmjd1a, Interacts With the Myocardin Factors to Regulate SMC Differentiation Marker Gene Expression. *Circulation Research* 101(12):e115-e123.
46. Gomez D, Shankman LS, Nguyen AT, & Owens GK (2013) Detection of histone modifications at specific gene loci in single cells in histological sections. *Nat Meth* 10(2):171-177.
47. Colussi C, *et al.* (2009) Nitric oxide deficiency determines global chromatin changes in Duchenne muscular dystrophy. *The FASEB Journal* 23(7):2131-2141.
48. Kouzarides T (2007) Chromatin modifications and their function. *Cell* 128(4):693-705.
49. Torella D, *et al.* (2011) MicroRNA-133 Controls Vascular Smooth Muscle Cell Phenotypic Switch In Vitro and Vascular Remodeling In Vivo. *Circulation Research* 109(8):880-893.
50. Dangwal S & Thum T (2014) microRNA Therapeutics in Cardiovascular Disease Models. *Annual Review of Pharmacology and Toxicology* 54(1):null.
51. Wei Y, Schober A, & Weber C (2013) Pathogenic arterial remodeling: the good and bad of microRNAs. *American Journal of Physiology - Heart and Circulatory Physiology* 304(8):H1050-H1059.
52. Li F, *et al.* (2010) Sonic Hedgehog Signaling Induces Vascular Smooth Muscle Cell Proliferation via Induction of the G1 Cyclin-Retinoblastoma Axis. *Arteriosclerosis, Thrombosis, and Vascular Biology* 30(9):1787-1794.
53. Gregory PA, *et al.* (2011) An autocrine TGF-β/ZEB/miR-200 signaling network regulates establishment and maintenance of epithelial-mesenchymal transition. *Molecular Biology of the Cell* 22(10):1686-1698.
54. Kumarswamy R, *et al.* (2012) Transforming Growth Factor-β–Induced Endothelial-to-Mesenchymal Transition Is Partly Mediated by MicroRNA-21. *Arteriosclerosis, Thrombosis, and Vascular Biology* 32(2):361-369.
55. Balderman JAF, *et al.* (2012) Bone Morphogenetic Protein-2 Decreases MicroRNA-30b and MicroRNA-30c to Promote Vascular Smooth Muscle Cell Calcification. *Journal of the American Heart Association* 1(6).
56. Díez M, Musri MM, Ferrer E, Barberà JA, & Peinado VI (2010) Endothelial progenitor cells undergo an endothelial-to-mesenchymal transition-like process mediated by TGFβRI. *Cardiovascular Research* 88(3):502-511.
57. Bhardwaj S, Roy H, Heikura T, & Ylä-Herttuala S (2005) VEGF-A, VEGF-D and VEGF-DΔNΔC induced intimal hyperplasia in carotid arteries. *European Journal of Clinical Investigation* 35(11):669-676.
58. Fu C, *et al.* (2012) Monocyte Chemoattractant Protein-1/CCR2 Axis Promotes Vein Graft Neointimal Hyperplasia Through Its Signaling in Graft-Extrinsic Cell Populations. *Arteriosclerosis, Thrombosis, and Vascular Biology* 32(10):2418-2426.
59. Cieslik KA, *et al.* (2011) Immune-inflammatory dysregulation modulates the incidence of progressive fibrosis and diastolic stiffness in the aging heart. *J Mol Cell Cardiol* 50(1):248-256.
60. Schepers A, *et al.* (2006) Anti–MCP-1 Gene Therapy Inhibits Vascular Smooth Muscle Cells Proliferation and Attenuates Vein Graft Thickening Both In Vitro and In Vivo. *Arteriosclerosis, Thrombosis, and Vascular Biology* 26(9):2063-2069.
61. Kranzhöfer A, Baker AH, George SJ, & Newby AC (1999) Expression of Tissue Inhibitor of Metalloproteinase-1, -2, and -3 During Neointima Formation in Organ Cultures of Human Saphenous Vein. *Arteriosclerosis, Thrombosis, and Vascular Biology* 19(2):255-265.
62. van Tiel CM & de Vries CJM (2012) NR4All in the vessel wall. *The Journal of Steroid Biochemistry and Molecular Biology* 130(3–5):186-193.
63. Newby AC (2013) Coronary vein grafting: the flags keep waving but the game goes on. *Cardiovascular Research* 97(2):193-194.

64. Batellier J, Wassef M, Merval R, Duriez M, & Tedgui A (1993) Protection from atherosclerosis in vein grafts by a rigid external support. *Arteriosclerosis, Thrombosis, and Vascular Biology* 13(3):379-384.
65. Berceli SA, *et al.* (2004) Differential expression and activity of matrix metalloproteinases during flow-modulated vein graft remodeling. *Journal of Vascular Surgery* 39(5):1084-1090.
66. Thum T, *et al.* (2008) MicroRNA-21 contributes to myocardial disease by stimulating MAP kinase signalling in fibroblasts. *Nature* 456(7224):980-984.
67. Neth P, Nazari-Jahantigh M, Schober A, & Weber C (2013) MicroRNAs in flow-dependent vascular remodelling. *Cardiovascular Research* 99(2):294-303.
68. Brønnum H, *et al.* (2013) miR-21 Promotes Fibrogenic Epithelial-to-Mesenchymal Transition of Epicardial Mesothelial Cells Involving Programmed Cell Death 4 and Sprouty-1. *PLoS ONE* 8(2):e56280.
69. Liu X, *et al.* (2009) A Necessary Role of miR-221 and miR-222 in Vascular Smooth Muscle Cell Proliferation and Neointimal Hyperplasia. *Circulation Research* 104(4):476-487.
70. Cavarretta E, Latronico MVG, & Condorelli G (2012) Endothelial-to-Mesenchymal Transition and MicroRNA-21: The Game Is On Again. *Arteriosclerosis, Thrombosis, and Vascular Biology* 32(2):165-166.
71. Wang YK, *et al.* (2011) Bone Morphogenetic Protein-2-Induced Signaling and Osteogenesis Is Regulated by Cell Shape, RhoA/ROCK, and Cytoskeletal Tension. *Stem cells and development*.
72. Gregory PA, *et al.* (2008) The miR-200 family and miR-205 regulate epithelial to mesenchymal transition by targeting ZEB1 and SIP1. *Nat Cell Biol* 10(5):593-601.
73. Magenta A, *et al.* (2011) miR-200c is upregulated by oxidative stress and induces endothelial cell apoptosis and senescence via ZEB1 inhibition. *Cell Death Differ* 18(10):1628-1639.
74. Reddy MA, *et al.* (2012) Pro-Inflammatory Role of MicroRNA-200 in Vascular Smooth Muscle Cells From Diabetic Mice. *Arteriosclerosis, Thrombosis, and Vascular Biology* 32(3):721-729.
75. McGeachie J, Campbell P, & Prendergast F (1981) Vein to artery grafts. A quantitative study of revascularization by vasa vasorum and its relationship to intimal hyperplasia. *Annals of surgery* 194(1):100-107.
76. Khurana R, *et al.* (2004) Angiogenesis-Dependent and Independent Phases of Intimal Hyperplasia. *Circulation* 110(16):2436-2443.
77. Tanaka K, *et al.* (2011) Augmented angiogenesis in adventitia promotes growth of atherosclerotic plaque in apolipoprotein E-deficient mice. *Atherosclerosis* 215(2):366-373.
78. Tigges U, Komatsu M, & Stallcup WB (2013) Adventitial pericyte progenitor/mesenchymal stem cells participate in the restenotic response to arterial injury. *Journal of vascular research* 50(2):134-144.

Chapter IV:

Summary

Conclusions

Future Perspectives

Summary of the thesis

Coronary artery bypass grafting (CABG) has been introduced in vascular surgery more than 50 years ago to fix the consequences of myocardial ischemia [1]. The two most represented coronary-compatible autologous vessels to be used in CABG are the inner mammary artery and the saphenous vein. The clinical impact of graft failure is different depending on the origin of vessel employed. It is estimated that mammary artery grafts maintain an 85% of patency after 10 years while patency of SV grafts drops to 50% at a comparable time. It became evident that the transplanted vessels are liable to undergo a series of structural modifications leading to significant patency reduction with the need of patient re-hospitalization, stent implantation or ultimately re-intervention [2]. Basic investigations have clarified the role of vascular-resident cells or recruited cells (inflammatory cells) on the establishment of intimal hyperplasia (IH). IH is the remodeling of vessel wall, progressively the uncontrolled proliferation of vascular resident cells leads to the narrowing of the lumen, causing ultimately vessel occlusion. The venous adaptive response to the arterial environment during the post-surgical process, is a distinctive property of the vein graft. Vascular remodeling in vein grafts is thought to be a normal and necessary response for environmental adaptation, commonly known as “arterialization”, e.g. to the high wall shear stress and stretch force. Since vein graft adaptation presents similar physiologic characteristics and clinical sequelae when compared to the post-arterial injury response, it is possible that VGD share the same underlying mechanism. Even the term “neointimal hyperplasia”, usually applied to pathological remodeling after arterial injury, has been extended to pathological excessive venous remodeling. Thus, uncovering the mechanisms underlying venous IH would be of help to identify biological mechanisms involved also in pathologic arterial injury, and *vice versa*. It is likely that vein graft adaptation has specific and distinct differences in its molecular mechanisms, e.g. those specific to venous cells, compared to those processes involved in arterial vessel wall remodeling after arterial injury.

Two major biomechanical components are believed to contribute to vein arterialization; these are the flow-related shear stress, which is increased in CABG due to a raise in flow velocity, and the wall stress/strain, which is also increased due to a switch from venous to arterial pressure [3].

The purpose of this doctoral thesis is to highlight the underlying physiological and molecular events involved in the early vein graft adaptation to the arterial-related pressure conditions. We have pursued this regard through a bioengineering approach in order to reproduce arterialization in cultured human veins. The system used has been devised to obtain original information on the effects of arterial-like wall strain on structural (Chapter II) and molecular (Chapter III) changes that predispose SV to remodeling events occurring after CABG transplantation.

Data indicated a clear thinning of the SV wall and a marked enlargement of the luminal perimeter, two parameters which have been found significantly changed during arterial positioning of vein segments in patients and animal models [1]. Interestingly, the cross-sectional area of the tissue (thus the mass of the vessel wall) did not change after 7 days of arterial-like pressure stimulation.

Significant decrease of cell density and significant increase in cellular proliferation rate were observed in SVs segments under arterial-like strain stimulation. These latter findings are in accordance with reports of Miyakawa [4] and Voisard [5], showing first signs of reactive cell proliferation after days. In addition, we observed a contribution of the CABG-PS to determine microscopic ruptures in the endothelial layer and a striking disarray in the SMCs layers in the medial tissue, two factors known to predispose the vessel to pathologic remodeling [6]. Exposure of SV segments to CABG-PS induced changes in the histones H3/H4 acetylation/methylation levels, especially in adventitial cells and cells of the *vasa vasorum*. This correlates with an increase in *vasa vasorum* length density (range 24-44 μm) and their structural disarrangement. The disorganization of *vasa vasorum* was also observed by IF analyses for αSMA and ECs markers in CABG-PS veins. MMP-2 and MMP-9 enzymes were found activated in both CABG-PS and VP conditions, but different expression of TIMP-1, a MMPs inhibitor, was observed in the two conditions. Molecular investigations showed a panel of various micro RNA and growth factors differentially expressed, some of these are specific for CABG-PS or VP, after the two culture conditions.

Conclusions

The ex vivo vein culture system (ECVS) adopted in this project has proved a valuable, reliable, easy handling and versatile tool for studying arterial pressure events triggered in VGD. This platform is therefore a novel laboratory-oriented tool that will be useful to carry out *ex vivo* culture campaigns under controlled hemodynamic conditions and dissect the contribution of biomechanical forces involved in the early IH priming in vein CABG.

The biological data achieved confirm an important contribution of the arterial-like wall strain in SV structural and biochemical changes, activation of vessel resident cells and in the expression of molecular signals involved in the pathogenesis of IH.
The stimulus of arterial pressure acting on vein grafts vessel wall induces the expression of various paracrine signals and intracellular signals, therefore targeting these molecules could be an effective way to control vein graft wall thickness. The ultimate goal of this project is to find a treatment that can prevent, avoid or reduce the incidence of the vein graft disease in patients subjected to CABG surgery with saphenous vein. This treatment could include one or more targets identified in this work focusing on the early stage of the pathological adaptation of the SV to the new hemodynamic environment.

Future Perspectives and Traslationality of the Project

Although there are numerous successful experimental treatments for vein graft wall thickening in animal models, no accepted strategy for management of vein graft neointimal hyperplasia has translated into clinical use.
The present project reaches important results that elucidate the role of pressure stimulation on vein graft pathogenesis. The achievements of this study are essential not only for clarifying the role of this biomechanical force but also, and above all, for their traslationality from basic research into the clinical medicine. Indeed, this project is part of a larger study on vein graft disease which aims to find an effective treatment for avoiding or preventing vein graft intimal hyperplasia. The purpose is to condition vein segments with a specific cocktail of factors, antibodies, antago-mir in order to inhibit

or enhance signals crucial for the development of uncontrolled cellular proliferation and deposition of matrix. Another possibility is to condition the vein segments with arterial mechanical forces using the EVCS; adopting this method vein adaptation to its new hemodynamic condition will take place ex vivo avoiding the release of molecular effectors that induce IH.

Moreover, these results paves the way to future basic science studies on the topic of biomechanical forces acting on venous vessels subjected to arterial stimuli. These studies will comprise for example, the assessment of the role of arterial shear stress, tissue hypoxia, sine-like pressure stimulation on IH. For these purposes novel biomimetic features were introduced into the existing EVCS. A better biomimicking of the arterial hematochemical environment was reached with the devise of a double–compartment ex vivo vessel culture system (DC-EVCS) by µBS Lab of Politecnico di Milano. This novel double culture system separates the culture medium that circulate in contact with the vessel lumen from that in contact with the outer portion. This feature provides a great advice: for instance, the possibility to expose the intimal and adventitial layer to two distinct solutions containing different factors. For this purpose, the DC-EVCS equipped with a deoxygenating circuit was dimensioned and manufactured for testing different luminal and adventitial oxygen concentration to simulate the hypoxic condition of vein grafts. To reproduce the best the CABG environment experienced by vein segments, the DC-EVCS was designed to expose the luminal and adventitial layer to different factors, in combination with the arterial-like pressure stimulation of vein segments. DC-EVCS may also contribute to study the role of different cell populations in the progression of intimal hyperplasia of vein graft by the injection of marked cells into the inner or outer circuit and following them during their fate.
The full hydrodynamic mechanical stimuli acting in CABG arterialization, *i.e.* pulsatile wall stretch and wall shear stress applied synchronously with the correct phasing, was reproduce by an upgrading of the DC-EVCS. Also this latter devise has been conceived and designed in collaboration with Politecnico di Milano.

Over the past 60 years, numerous physiologic and molecular mechanisms of vein graft adaptation have been discovered. However, this complex process has yet to be clarified, and we do not have the ability to therapeutically

control graft wall thickening. A great scientific effort remains to carry out before the complete understanding of vein graft disease will be achieved.

As described into the Introduction section, VGD is a complex pathologic system in which multiple factors, cell types, paracrine and intracellular signals occur. Surgical handling, endothelial denudation, inflammation, SMCs switching phenotype, altered hemodynamic forces are the actors of a complicated play script. The use of ex vivo bio-engineering approach permits to study this pathology dissecting the complex system, thus, studying the role of every element alone.

The present work made a little step to understand IH pathophysiology, but a long path had to be walked before reaching our final aim, the one to expose directly the explanted vein to the conditioning treatment on the back table of the operating room prior to surgical implantation of the treated vein.

References

1. Owens, C.D., *Adaptive changes in autogenous vein grafts for arterial reconstruction: clinical implications.* J Vasc Surg, 2010. **51**(3): p. 736-46.
2. Parang, P. and R. Arora, *Coronary vein graft disease: pathogenesis and prevention.* Can J Cardiol, 2009. **25**(2): p. e57-62.
3. John, L.C., *Biomechanics of coronary artery and bypass graft disease: potential new approaches.* Ann Thorac Surg, 2009. **87**(1): p. 331-8.
4. Miyakawa, A.A., et al., *Human saphenous vein organ culture under controlled hemodynamic conditions.* Clinics (Sao Paulo), 2008. **63**(5): p. 683-8.
5. Voisard, R., et al., *Pulsed perfusion in a venous human organ culture model with a Windkessel function (pulsed perfusion venous HOC-model).* Med Sci Monit, 2010. **16**(11): p. CR523-9.
6. Motwani, J.G. and E.J. Topol, *Aortocoronary saphenous vein graft disease: pathogenesis, predisposition, and prevention.* Circulation, 1998. **97**(9): p. 916-31.

Publications

PEER-REVIEWED PUBLICATIONS

- A compact and automated ex vivo vessel culture system for the pulsatile pressure conditioning of human saphenous veins. Piola M, **Prandi F**, Bono N, Soncini M, Penza E, Agrifoglio M, Polvani G, Pesce M, Fiore GB. *J Tissue Eng Regen Med*. 2013 Jul 30

- Mechanical compliance and immunological compatibility of fixative-free decellularized/cryopreserved human pericardium. Vinci MC, Tessitore G, Castiglioni L, **Prandi F**, Soncini M, Santoro R, Consolo F, Colazzo F, Micheli B, Sironi L, Polvani G, Pesce M. *PLoS One*. 2013 May 21;8(5):e64769

- Tools and procedures for ex vivo vein arterialization, preconditioning and tissue engineering: a step forward to translation to combat the consequences of vascular graft remodeling. Piola M, Soncini M, **Prandi F**, Polvani G, Beniamino Fiore G, Pesce M. *Recent Pat Cardiovasc Drug Discov.* 2012 Dec;7(3):186-95. Review

- Endothelial and cardiac progenitors: boosting, conditioning and (re)programming for cardiovascular repair. Pesce M, Burba I, Gambini E, **Prandi F**, Pompilio G, Capogrossi MC. *Pharmacol Ther*. 2011 Jan;129(1):50-61. Review

BOOK CHAPTER

- Natural Membranes as Scaffold for Biocompatible Aortic Valve Leaflets: Perspectives from Pericardium. Vinci MC, **Prandi F**, Micheli B, Tessitore G, Guarino A, Dainese L, Polvani G, Pesce M. *Biomaterials and Stem Cells in Regenerative Medicine*. ISBN: 978-1-4398-7925-2